TISSUE ENGINEERING STRATEGIES FOR THE RECONSTRUCTION OF A FUNCTIONAL LARYNX

by

Sarah Elizabeth Brookes, D.V.M.

A Dissertation

Submitted to the Faculty of Purdue University

In Partial Fulfillment of the Requirements for the degree of

Doctor of Philosophy

Department of Basic Medical Sciences

West Lafayette, Indiana

May 2021

THE PURDUE UNIVERSITY GRADUATE SCHOOL
STATEMENT OF COMMITTEE APPROVAL

Dr. Sherry Harbin, Chair
Weldon School of Biomedical Engineering

Department of Basic Medical Sciences

Dr. Stacey Halum
I.U. School of Medicine

Dr. Marxa Figueiredo
Department of Basic Medical Sciences

Dr. Russell Main
Department of Basic Medical Sciences

Weldon School of Biomedical Engineering

Approved by:
Dr. Laurie Jaeger

This is dedicated to my daughters Arianna and Willow who have watched me grow as a scientist as I have watched them grow as humans.

ACKNOWLEDGMENTS

This project was supported in part by award number R01DC014070-01A1 from the National Institute on Deafness and Other Communication Disorders (NIDCD) within the National Institutes of Health (NIH).

Without the following people, none of this work would have been possible:

I would like to thank Hongji Zhang for her work in creating and engineering the cartilage implants for the rat studies; Lujuan Zhang for her work in scaling up the cartilage implants for the pig studies, as well as performing all of the PCR work; TJ Puls and Geniphys for manufacturing the collagen oligomer and designing and creating the cartilage and mucosa implants. I would also like to thank the BME animal tech team for their incredible assistance with all of the animal studies. Rat surgeries were performed by Stacey Halum, Hongji Zhang, and me. Pig surgeries were performed primarily by Stacey Halum with me assisting.

TABLE OF CONTENTS

ABSTRACT

Laryngeal cancer affects tens of thousands worldwide every year. The standard of care of surgical resection, chemotherapy, and/or radiation therapy results in significant quality of life deficits including reliance on tracheostomy tubes, loss of voice, and inability to swallow. There are no therapeutic options that restore a functional larynx so that patients can live a more normal life. Laryngeal reconstruction using tissue engineering strategies offers the potential to solve this problem. Laryngeal anatomy is complex with multiple tissue types and therefore engineering approaches require consideration of a multi-layer, interfacial tissue design. Our strategy to overcome these challenges involves the use of advanced bio fabrication techniques where type I oligomeric collagen alone or in the presence of autologous stem cells is used to custom-make the cartilage, skeletal muscle, and mucosal layer of the larynx. This doctoral research project begins by describing the development of the tissue engineered skeletal muscle with aligned collagen matrix and autologous muscle progenitor cells induced to express motor endplates. Next, using this engineered muscle plus the cartilage layer developed by a colleague; we implanted the myochondral engineered construct in a rat hemilaryngectomy model. In this study we saw host-implant integration with no inflammatory foreign body response, neo cartilage and muscle formation, and some return of laryngeal function on the reconstructed side. Next, we worked to scale-up these technologies for use in a porcine model. The pig larynx is more similar in size and function to the human larynx and allows for a full thickness defect to be created. Using confined compression, we created 4-mm thick acellular and cellular cartilage constructs, as well as a 0.5-mm thick acellular mucosal layer. A 1-cm diameter muscle layer containing autologous muscle progenitor cells was created using flow alignment and cultured to induce expression of motor endplates before implantation. Tissue constructs were subjected to mechanical property analyses as well as PCR analysis to describe the differential gene expression by component cells within muscle and cartilage constructs. Each layer was individually sutured into a pig hemilaryngectomy model. The pigs recovered well from the surgery, were eating, had no difficulty breathing, and no aspiration events. At 2 months, respiratory epithelium had completely healed over the implant and was vascularized and had areas of submucosal gland growth. The motor endplate expressing muscle implants showed new, organized muscle ingrowth while the acellular implants showed a relative paucity of new, disorganized muscle.

This work represents a significant advancement in the field of laryngeal reconstruction and is a first of its kind to use scalable tissue engineering technologies designed to specifically meet each layer's functional criteria.

CHAPTER 1. INTRODUCTION

Laryngeal cancer is one of the most commonly diagnosed airway cancers, with over 13,000 new cases diagnosed and an estimated 3,750 deaths reported annually in the United States alone.[1] Most often, laryngeal cancer represents squamous cell carcinoma that affects cells lining the airway (Figure. 1.1). When identified at an early-stage, cancers are primarily treated with surgical resection, radiation therapy, or a combination of the two. However, as the cancer progresses, it invades the underlying skeletal muscle and cartilage and can progress to block the airway. It is these advanced stage, invasive tumors that require a more aggressive treatment, including surgical removal of all or part of the larynx (total or hemi-laryngectomy), which is often performed in combination with chemo and/or radiation therapy. The result is a five-year survival rate of 60-80% depending on the stage of cancer at the time of diagnosis.[1] Unfortunately, as a consequence of these life-saving but incredibly invasive treatments, patients suffer significant decreases in quality of life. This includes, but is not limited to, severe voice impairment or loss of voice entirely, disfiguring tracheostomy tubes or stomas, and an inability to swallow.[2] It is these negative sequelae that motivate the search for new therapeutic options to predictably restore laryngeal anatomy and function following tumor resection, bringing improved quality of life for cancer survivors and reducing over medical care costs.

Laryngeal transplants offer the possibility of restoring a functional larynx. Keeping all structures intact and restoring blood flow and innervation would, in theory, allow for a return to function. Based on this concept, the first transplant on a patient with laryngeal cancer was performed in 1969. However, the required immunosuppression contributed to rapid regrowth of the cancer and patient death,[3] therefore causing transplantation to be widely abandoned as an investigational treatment option for laryngeal cancer patients. In recent decades, scientists have turned to different options for laryngeal reconstruction. In order to fully understand the challenge of reconstructing a functional larynx, one must first look at the complexities of the organ's structure and function.

The larynx is anatomically complex and, as an organ, serves multiple vital functions from breathing to speaking to swallowing. The bulk and structure of the larynx is composed of six different cartilages attached together by a number of various muscles and ligaments. The thyroid and cricoid, which represent the largest cartilage components, form the primary structure of the

larynx and are composed of hyaline cartilage. The paired arytenoid cartilages, also of the hyaline variety, provide an anchor for the vocal folds and muscles that move them. The epiglottis is composed of elastic cartilage and plays a vital role in covering the airway during swallowing to prevent aspiration. The airway lining is made up of mucous membrane composed primarily of ciliated stratified squamous epithelium. This mucous membrane creates two folds extending into the airway. The first are the vestibular folds, more commonly referred to as the false vocal cords due to the fact that they do not contribute to phonation (voice production). Under the false cords are the true vocal cords and these are responsible for phonation. The structure of the vocal cords is vital to their function in phonation, airway protection, and respiration. Each vocal cord is composed of multiple layers: a stratified squamous epithelium that serves as a protective barrier. Underneath this epithelial layer is the superficial, intermediate, and deep lamina propria. The superficial lamina propria, also referred to as Reinke's space, provides the vibratory characteristics of the vocal folds and is composed of a loose matrix of type I collagen, elastin, and reticular fibers with interspersed glycosaminoglycans (GAGs)[4]. The intermediate and deep layers are composed of elastin and collagen fibers respectively and function as a transition and attachment zone for the vocal fold mucosa to the underlying thyroarytenoid muscle. The muscles of the larynx can be divided into those responsible for respiration and those responsible for phonation. The main respiratory muscle is the posterior cricoarytenoid which abducts, or opens up, the vocal folds to allow for breathing. The phonatory muscles act to adduct, or bring together, the vocal folds to vibrate and produce sound and consist, primarily, of the thyroarytenoid, lateral cricoarytenoid, interarytenoid, and cricothyroid muscles. (Figure 1.1) These muscles also orchestrate the adduction (laryngeal closure) needed to produce an efficient cough and to protect the airway during swallowing. Innervation to virtually all the laryngeal musculature, with the exception of the cricothyroid muscle, is by the recurrent laryngeal nerve (RLN), a branch of the vagus nerve. The cricothyroid muscle is innervated by the external branch of the superior laryngeal nerve (a separate branch of the vagus nerve).

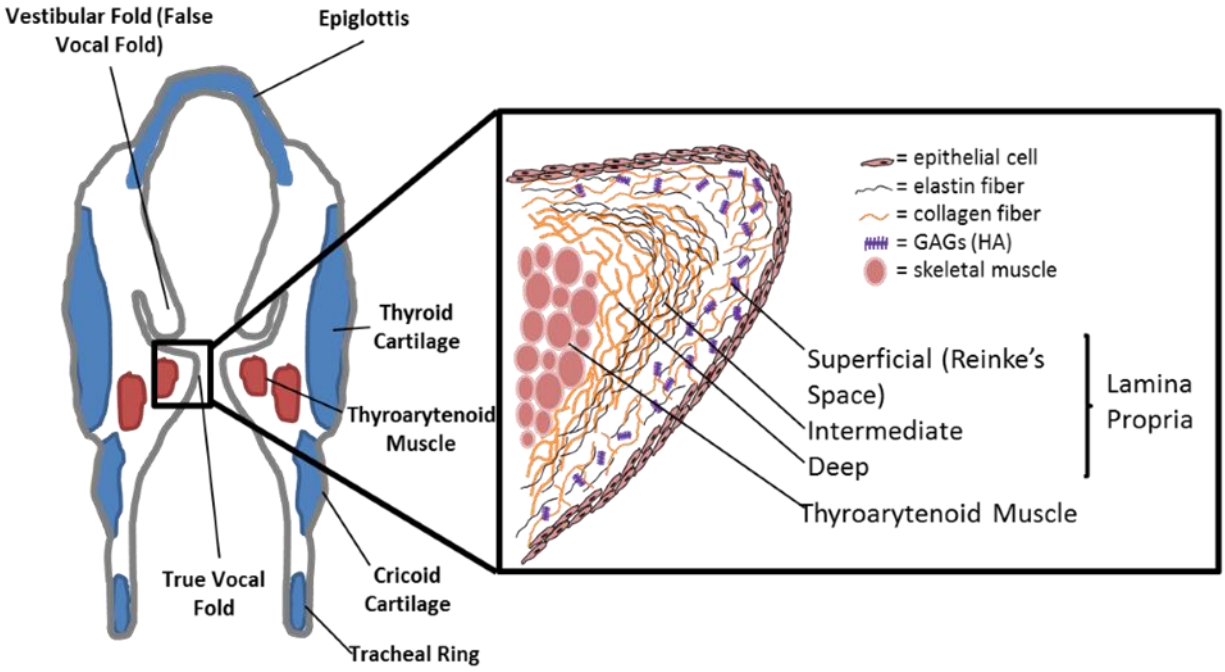

Figure 1.1: Longitudinal cross-section of laryngeal anatomy with associated higher resolution image of vocal fold micro-anatomy.

There are currently no therapeutic strategies to restore dynamic laryngeal function post laryngectomy. The current surgical standard of care is the use of autologous grafts, such as myocutaneous flaps and buccal mucosa to surgically close the tissue void following tumor resection. While these replacement tissues provide some structure, they are bulky, come with donor site availability and morbidity problems, and do not restore any dynamic function.[2] A recent review by Hamilton et al. indicated that a potential treatment strategy for advanced laryngeal cancer is to tissue engineer a functional autologous laryngeal replacement.[2] A laryngeal replacement fabricated using autologous cells obviates the need for immune suppression, thereby avoiding the increased risk of tumorigenesis which was seen with the first laryngeal transplant.[5] An autologous laryngeal replacement can include a number of design considerations including restoration of i) structure through scaffold design and ii) function by promoting skeletal muscle regeneration with associated vascularization and innervation. Approaches aimed at recapitulating laryngeal structure have included using decellularized larynx[6], decellularized cartilage[7], or various natural and synthetic biomaterials seeded with cells.[4,8–12] Major limitations of these approaches have been: inadequate integration with the

surrounding host tissue, significant inflammatory response, and poor vascularization/tissue survival, and no return of function.

Another vital, but often overlooked, component to restoring laryngeal function is replacing and/or regenerating skeletal muscle and nerve components. Skeletal muscle tissue engineering is a very active area of research that is mainly aimed at treating volumetric muscle loss (VML) and muscular dystrophies. However, these advanced tissue engineering and regenerative strategies may also provide otolaryngologists with new tools and approaches for restoring laryngeal function. To achieve maximum therapeutic benefit, it has been proposed that engineered muscle should 1) be constructed from autologous cell sources; 2) recapitulate the structure and functional properties of native skeletal muscle, which represents aligned muscle fibers interfacing within an appropriate, well-organized extracellular matrix (ECM); 3) integrate rapidly into host tissue with associated neovascularization and innervation; and 4) support scalable and patient-specific design.[13,14] Although significant advances have been made in achieving this goal, persistent shortcomings remain, especially those related to scalable fabrication and identification of standardized and customizable natural biomaterials, which effectively recapitulate the guiding interface between muscle and its ECM and accelerate interfacial tissue regeneration.

Evaluation of the hierarchical structure–function of skeletal muscle reveals an intricate tissue design, including muscle fibers, with their associated contractile machinery and a rich neurovascular supply, which are essential for inducing and sustaining dynamic contraction. Furthermore, muscle ECM plays a critical role in guiding the muscle–nerve–vascular interface, as well as supporting muscle's mechanical function, adaptability, and repair.[15] Therefore; it is not surprising that the majority of muscle engineering approaches focus on capturing these essential design features.

At present, the most widely used cell source for engineering skeletal muscle is the putative muscle progenitor cell (satellite cell; MPC), which readily can be isolated from muscle biopsies and cultured to produce myoblasts.[16] However, many additional cell sources have been investigated including induced pluripotent stem cells[17], bone marrow mesenchymal stem cells[18], and adipose stem cells.[19,20] Major considerations in choice of cell source include: donor site morbidity, expansion capacity, differentiation potential, compatibility in vivo, and potential

tumorgenicity. In turn, these cells are interfaced with a variety of natural and synthetic biomaterials designed to promote myoblast fusion, differentiation, and maturation *in vitro*.

Synthetic polymers, such as polycaprolactone, polyethylene glycol (PEG), polyurethane, and poly(lactic-co-glycolic) acid, often are the engineering material of choice, largely owing to their mechanical stability, design versatility, and amenability to micro- and nano-fabrication techniques (e.g., electrospinning, patterning).[21] They are limited, however, by their lack of cell adhesion sites/bioactivity often requiring the addition of a natural biomaterial. Additionally, upon implantation *in vivo*, these materials are sensed as "foreign" by the body, yielding an inflammatory-mediated, foreign-body response.[22]

Decellularized tissues (e.g., skeletal muscle), which are processed to maintain the complex composition, structural integrity, and architectural features of tissue ECM while eliminating immunogenic cellular components, have also been applied.[22] However, these graft materials induce an inflammatory reaction as well, and their dense microstructure prevents complete recellularization and restoration of muscle function.[23] As an alternative, natural or nature-derived polymers such as fibrin, type I collagen, laminin, keratin, hyaluronic acid, silk, or gelatin have been used alone or in combination.[20,24–27] For these applications, cell-matrix constructs are cast within silicone or polydimethylsiloxane molds to form cylindrical or rectangular-shaped constructs. Constructs are then anchored at each end to provide passive tension, which is known to promote unidirectional cell alignment and fusion.[26] Although it is evident that these natural materials provide essential cell adhesion sites and associated bioinstructive properties, they are known to exhibit high batch-to-batch variability, require exogenous cross-linking, and are less amenable to the control of their physicochemical properties than synthetic polymers.[13] In recent years, more elegant designs have been created that include multiple cell types, pre-vascularization, and pre-innervation all with reported improvements in functional outcomes in VML studies.[22] However, these more complex designs pose significant challenges in terms of scalable manufacturing and regulatory approval. Collectively, these strategies involving synthetic and natural materials have resulted in significant advancements with respect to muscle engineering; however, the search continues for a next-generation muscle design that has morphological similarities to native muscle, supports rapid differentiation and maturation in vitro, has suitable mechanical integrity for handling, and rapid functional integration and neurovascular regeneration following implantation within the body.

Our efforts directed at providing new and improved laryngeal tissue restoration have focused on the use of a polymerizable collagen formulation, known as type I oligomeric collagen, which is fabricated in the presence and absence of autologous stem or progenitor cell populations. The focus of the first aim of this project has been on creating a skeletal muscle implant that meets the design criteria mentioned above. Additional work performed by colleagues Hongji Zhang and Lujuan Zhang has focused on development of the cartilage implant using densified collagen oligomer and adipose stem cells.[28] Finally, enabling contributions by T.J. Puls and GeniPhys have led to the development of prototype high-strength collagen material for reconstruction of mucosal layer of the larynx.

1.1 Thesis Organization

The material in this thesis represents our efforts and progress aimed at the development of a tissue engineered larynx to restore dynamic laryngeal function as there are no current clinical options. The application of type I collagen oligomer, autologous stem cells, and the advanced fabrication techniques of flow alignment and confined compression, has allowed us to develop and evaluate early prototypes of engineered cartilage, muscle, and mucosa constructs for laryngeal restoration in rodent and porcine animal models.

The introductory chapter largely represents material from my Preliminary Examination. Chapter 2 was published in The Laryngoscope in 2018 and addresses the in vitro characterization of the skeletal muscle implant and implantation into a rat model.

Chapter 3 was published in The Laryngoscope in 2019 and addresses the implantation of both the skeletal muscle and cartilage implants in a rat model, along with analysis of the return of function after nerve injury and laryngeal reconstruction.

Chapter 4 was published in The Laryngoscope in 2020 and represents a proof-of-concept study demonstrating the size scaling of these constructs for use in a pig model. This pilot study involved creation of full-thickness transmural defects in the larynx of pigs followed by a three-layer reconstruction approach involving prototype mucosa, muscle, and cartilage layers.

Lastly, in Chapter 5 we summarize our findings and discuss their significance, along with proposing plans for future work.

1.2 References:

1. SEER laryngeal cancer stats.
2. Hamilton, N. J. I. & Birchall, M. A. Tissue-Engineered Larynx: Future Applications in Laryngeal Cancer. Curr. Otorhinolaryngol. Rep. 5, 42–48 (2017).
3. Kluyskens, P. & Ringoir, S. Follow-up of a human larynx transplantation. The Laryngoscope 80, 1244–1250 (1970).
4. Long, J. L. Repairing the vibratory vocal fold: Repairing the Vibratory Vocal Fold. The Laryngoscope 128, 153–159 (2018).
5. Krishnan, G. et al. The current status of human laryngeal transplantation in 2017: A state of the field review: Human Laryngeal Transplantation in 2017. The Laryngoscope 127, 1861–1868 (2017).
6. Herrmann, P. et al. In vivo implantation of a tissue engineered stem cell seeded hemi-laryngeal replacement maintains airway, phonation, and swallowing in pigs. J. Tissue Eng. Regen. Med. (2017) doi:10.1002/term.2596.
7. Macchiarini, P. et al. Clinical transplantation of a tissue-engineered airway. 372, 8 (2008).
8. Kitamura, M. et al. Glottic regeneration with a tissue-engineering technique, using acellular extracellular matrix scaffold in a canine model: Glottic regeneration with an acellular scaffold. J. Tissue Eng. Regen. Med. 10, 825–832 (2016).
9. Wambach, B. A., Cheung, H. & Josephson, G. D. Cartilage Tissue Engineering Using Thyroid Chondrocytes on a Type I Collagen Matrix: The Laryngoscope 110, 2008–2011 (2000).
10. Kitani, Y. et al. Laryngeal Regeneration Using Tissue Engineering Techniques in a Canine Model. Ann. Otol. Rhinol. Laryngol. 120, 49–56 (2011).
11. Fukahori, M. et al. Regeneration of Vocal Fold Mucosa Using Tissue-Engineered Structures with Oral Mucosal Cells. PLOS ONE 11, e0146151 (2016).
12. Ling, C. et al. Bioengineered vocal fold mucosa for voice restoration. Sci. Transl. Med. 7, 314ra187-314ra187 (2015).
13. Juhas, M. & Bursac, N. Engineering skeletal muscle repair. Curr. Opin. Biotechnol. 24, 880–886 (2013).

14. Mertens, J. P., Sugg, K. B., Lee, J. D. & Larkin, L. M. Engineering muscle constructs for the creation of functional engineered musculoskeletal tissue. Regen. Med. 9, 89–100 (2014).
15. Gillies, A. R. & Lieber, R. L. Structure and function of the skeletal muscle extracellular matrix. Muscle Nerve n/a-n/a (2011) doi:10.1002/mus.22094.
16. Cheng, C. S., Davis, B. N., Madden, L., Bursac, N. & Truskey, G. A. Physiology and metabolism of tissue-engineered skeletal muscle. Exp. Biol. Med. 239, 1203–1214 (2014).
17. Rao, L., Qian, Y., Khodabukus, A., Ribar, T. & Bursac, N. Engineering human pluripotent stem cells into a functional skeletal muscle tissue. Nat. Commun. 9, 126 (2018).
18. Merritt, E. K. et al. Repair of traumatic skeletal muscle injury with bone-marrow-derived mesenchymal stem cells seeded on extracellular matrix. Tissue Eng. Part A 16, 2871–2881 (2010).
19. Kesireddy, V. Evaluation of adipose-derived stem cells for tissue-engineered muscle repair construct-mediated repair of a murine model of volumetric muscle loss injury. Int. J. Nanomedicine 11, 1461–1473 (2016).
20. Gilbert-Honick, J. et al. Adipose-derived Stem/Stromal Cells on Electrospun Fibrin Microfiber Bundles Enable Moderate Muscle Reconstruction in a Volumetric Muscle Loss Model. Cell Transplant. 27, 1644–1656 (2018).
21. Ostrovidov, S. et al. Skeletal Muscle Tissue Engineering: Methods to Form Skeletal Myotubes and Their Applications. Tissue Eng. Part B Rev. 20, 403–436 (2014).
22. Gilbert-Honick, J. & Grayson, W. Vascularized and Innervated Skeletal Muscle Tissue Engineering. Adv. Healthc. Mater. 9, e1900626 (2020).
23. Porzionato, A. et al. Decellularized Human Skeletal Muscle as Biologic Scaffold for Reconstructive Surgery. Int. J. Mol. Sci. 16, 14808–14831 (2015).
24. Hinds, S., Bian, W., Dennis, R. G. & Bursac, N. The role of extracellular matrix composition in structure and function of bioengineered skeletal muscle. Biomaterials 32, 3575–3583 (2011).
25. Rhim, C. et al. Morphology and ultrastructure of differentiating three-dimensional mammalian skeletal muscle in a collagen gel. Muscle Nerve 36, 71–80 (2007).

26. Powell, C. A., Smiley, B. L., Mills, J. & Vandenburgh, H. H. Mechanical stimulation improves tissue-engineered human skeletal muscle. Am. J. Physiol.-Cell Physiol. 283, C1557–C1565 (2002).
27. Juhas, M. & Bursac, N. Roles of adherent myogenic cells and dynamic culture in engineered muscle function and maintenance of satellite cells. Biomaterials 35, 9438–9446 (2014).
28. Zhang, H. et al. Use of autologous adipose-derived mesenchymal stem cells for creation of laryngeal cartilage: ASCs for Creation of Laryngeal Cartilage. The Laryngoscope 128, E123–E129 (2018).

CHAPTER 2. THREE-DIMENSIONAL TISSUE-ENGINEERED SKELETAL MUSCLE FOR LARYNGEAL RECONSTRUCTION

Chapter 2 represents an article published in The Laryngoscope, 128:603–609, 2018

2.1 Introduction

Compromised laryngeal function, whether due to congenital malformations, trauma, cancer, or surgical defects, affects thousands of individuals worldwide each year.[1] Unfortunately, therapeutic options to restore lost muscle and dynamic laryngeal functions for these patients are limited. As a result, patients suffer devastating quality of life consequences, including severe voice impairment, an ineffective or unsafe swallow, or airway obstruction, often necessitating gastrostomy and/or tracheostomy tubes. Advanced tissue engineering and regenerative strategies aimed to develop skeletal muscle implants may provide clinicians with new tools and therapeutic strategies for treating these patients. To achieve maximum therapeutic benefit, it has been proposed that engineered muscle should 1) be constructed from autologous cell sources, 2) recapitulate the structure and functional properties of native skeletal muscle, which represents aligned muscle fibers interfacing within an appropriate, well-organized extracellular matrix (ECM), 3) integrate rapidly into host tissue with associated neovascularization and innervation, and 4) support scalable and patient-specific design.[2,3] While significant advances have been made in achieving this goal, persistent shortcomings remain, especially related to identification of standardized and customizable natural biomaterials which effectively recapitulate the guiding interface between muscle and its ECM and accelerate interfacial tissue regeneration.

Evaluation of the hierarchical structure-function of skeletal muscle reveals an intricate tissue design, including muscle fibers with their associated contractile machinery and a rich neurovascular supply which is essential for inducing and sustaining dynamic contraction. Furthermore, muscle ECM plays a critical role in guiding the muscle-nerve-vascular interface as well as supporting muscle's mechanical function, adaptability, and repair.[4] Therefore, it is not surprising that the majority of muscle engineering approaches focus on capturing these essential design features. At present, the most widely used cell source for engineering skeletal muscle is the putative muscle progenitor cell (MPC; satellite cell), which can be readily isolated from

muscle biopsies and cultured to produce myoblasts.[5] In turn, these cells are interfaced with a variety of natural and synthetic biomaterials, designed to promote myoblast fusion, differentiation, and maturation in vitro.

Synthetic polymers, including polycaprolactone and poly(lactic-co-glycolic) acid, are often the engineering material of choice largely owing to their mechanical stability, design versatility, and amenability to micro- and nano-fabrication techniques (e.g., electrospinning, patterning).[6] Unfortunately, upon implantation in vivo, these materials are sensed as "foreign" to cells, yielding an inflammatory-mediated, foreign-body response.[7,8] Decellularized tissues (e.g., skeletal muscle), which are processed to maintain the complex composition, structural integrity, and architectural features of tissue ECM, have also been applied. However, these graft materials also induce an inflammatory reaction, and their dense microstructure prevents complete recellularization and muscle recovery.[9] As an alternative, natural polymers, such as fibrinogen, type I collagen and Matrigel alone or in combination have been employed.[10-13] For these applications, cell-matrix constructs are cast within silicone or polydimethylsiloxane molds to form cylindrical or rectangular-shaped constructs. Constructs are then anchored at each end to provide passive tension, which is known to promote unidirectional cell alignment and fusion.[14] Although it is evident that these natural materials provide essential cell adhesion sites and associated bioinstructive properties, they are known to exhibit high batch-to-batch variability and are less amenable to the control of their physicochemical properties than synthetic polymers.[2] Although these strategies involving synthetic and natural materials have resulted in significant advancements with respect to muscle engineering, the search continues for a next-generation muscle design that harnesses myogenesis outside the body and rapid functional integration and neurovascular regeneration following implantation within the body.

The present work represents the first step towards a fabrication strategy for patient-specific human laryngeal muscle, featuring 1) alignment of component MPCs and a collagen-fibril ECM immediately upon fabrication and 2) induction of motor endplate expression to accelerate innervation following in-vivo implantation.[7] Fabrication involved interfacing MPCs with collagen-fibril matrices formed with type I collagen oligomers, an uncommon soluble collagen subdomain which retains natural intermolecular crosslinks.[15-17] Oligomers are ideally suited for tissue engineering and regeneration strategies since they 1) exhibit rapid suprafibrillar self-assembly yielding highly interconnected collagen-fibril matrices resembling those found in

vivo; 2) are standardized based upon their fibril-forming capacity; 3) support cell encapsulation and distribution throughout the construct; and 4) allow customized multi-scale design across the broadest range of tissue architectures and physical properties.[18] Published work shows that oligomer-encapsulated cells remain viable and respond to local matrix mechanophysical cues displaying altered morphology, cytomechanics, phenotype, and tissue morphogenesis.[15,19] Additional in-vivo studies have shown that the collagen-fibril material persists, inducing neovascularization, innervation, and little to no inflammatory response.[20,21]

In the current study, preliminary design optimization studies were performed assessing the effect of flow-alignment, MPC density, and collagen-matrix stiffness on MPC fusion and myotube formation in vitro. In turn, optimized muscle constructs prepared with MPCs or motor endplate expressing MPCs (MEEs) were then evaluated for their ability to restore muscle and cartilaginous hemilaryngeal defects in rats. We hypothesized that aligned MEE-oligomer constructs would contribute to rapid tissue integration and innervation in the absence of significant inflammatory reaction. Collectively, the integration of our knowledge and toolkits related to laryngeal reconstruction, standardized polymerizable collagens, and therapeutic muscle cell populations will provide important new insights towards achieving tissue-engineered muscle constructs for functional laryngeal restoration.

2.2 Materials and Methods

2.2.1 Myoblast Cell Line and Primary MPCs

C2C12 mouse myoblasts (ATCC, Rockville, Maryland) were cultured in Dulbecco's Modified Eagle Medium (DMEM; Fisher Scientific, Chicago, IL) supplemented with 1% penicillin, streptomycin, amphotericin B (PSF-1; HyClone, Logan, UT), and 10% fetal bovine serum (HyClone; Logan Utah) at 37^{o}C and 5% CO_2 . Cells were cultured to 70% confluency and used in experiments at passages 5 through 8. Primary MPCs were generated from skeletal muscle biopsies obtained from 12-week-old male Fischer 344 rats (Envigo, Indianapolis, IN) as previously described.[7] In brief, fresh muscle tissue was placed in myogenic growth medium (MGM), which consisted of DMEM supplemented with 1% PSF-1, 20% fetal bovine serum, and 0.1% chick embryo extract (Accurate Chemicals, Westbury, NY). Muscle was minced and digested in 0.2% collagenase type I (EMD Millipore, Temecula, CA) at 37°C for 2 hours.

Digested tissue was filtered through a 100μm cell strainer and washed 3 times with MGM. Resulting muscle fibers were suspended in MGM, plated onto untreated 100mm petri dishes (Fisher Scientific), and cultured overnight at 37°C within a humidified environment of 5% CO_2 in air. The supernatant was removed the next morning and transferred to culture flasks (Corning Life Sciences, Corning, NY). Cells were cultured to 70% confluency and used in experiments at passages 3 to 5.

2.2.2 Fabrication of Engineered Skeletal Muscle Constructs

Type I collagen oligomers were acid-solubilized from the dermis of market-weight pigs and lyophilized for storage as described previously.[15] The oligomer formulation was standardized on the basis of molecular composition as well as polymerization capacity according to ASTM International standard F3089-14.[22] Here the polymerization capacity is defined by the matrix shear storage modulus, G' (in Pa), as a function of oligomer concentration in the polymerization reaction. Each collagen solution was diluted with 0.01 N HCl to achieve the desired concentration. Neutralized solutions were kept on ice prior to induction of polymerization by warming to 37°C.

C2C12 cells or MPCs were suspended in neutralized oligomer collagen solution at either 1×10^6 or 1×10^7 cells/mL. The collagen-cell suspension (500μL) was injected into a pre-warmed 4-mm diameter Ultem (McMaster-Carr, Chicago, IL) cylinder mold and then allowed to polymerize at 37°C for 10 minutes. Immediately following polymerization, the construct was transferred to a customized culture chamber and secured with hook and loop fastener. Constructs were cultured in DMEM supplemented with 10% fetal bovine serum and 1% PSF-1 for 5 days with medium changes every 2 days. On day 5, medium was changed to differentiation medium, representing DMEM supplemented with 8% horse serum (HyClone) and 1% PSF-1, and constructs were cultured for an additional 7 days to induce myotube formation.

For a subset of experiments, MPCs were induced to express motor endplates (MEE) as described previously.[7] Briefly, muscle constructs were allowed to differentiate for 5 days at which point acetylcholine chloride (40 nM; Tocris Bioscience, Bristol, England), agrin (10 nM; R&D Systems, Minneapolis, Minnesota), and neuregulin (2 nM; R&D Systems) were added to the medium. Constructs were cultured an additional 7 days with medium changes every 3 days.

Motor endplate expression was confirmed by immunostaining with Alexa Fluor 594 conjugated α-bungarotoxin (Molecular Probes, Eugene, Oregon).

2.2.3 Laryngectomy and Implantation of Engineered Muscle

Engineered muscle constructs were evaluated in our established rat partial laryngectomy model.[8] The animal study protocol was approved by Purdue Animal Care and Use Committee (PACUC). Institutional guidelines, in accordance with the National Institutes of Health guidelines, were followed for the handling and care of the animals. In brief, 12 Fisher 344 rats were anesthetized with intraperitoneal injection of xylazine and ketamine and then maintained on 1% to 4% isoflurane. The ventral larynx was exposed via a midline incision. The sternohyoid muscle was incised and reflected to expose the thyroid cartilage. A relatively large section of hemithyroid cartilage and associated adductor muscle was removed from the left side. Animals were randomized into the following experimental groups: MPC-oligomer construct (n=4), MEE-oligomer construct (n=4), oligomer construct only (n=2), and defect only control (n=2). The construct was then placed into the defect (similar to a medialization laryngoplasty implant), with extrusion prevented by suturing overlying sternohyoid muscles to one another over the cartilaginous defect. Next, the subcutaneous tissue and skin were closed with 5-0 Vicryl (Medicon, Montreal, Quebec, Canada) suture.

2.2.4 Laryngeal Electromyography (EMG)

At 1-month and 3-month endpoints, laryngeal electromyography (EMG) was performed under anesthesia as previously described.[14] Electromyogram (Niking Viking Quest electromyography machine, Madison, Wisconsin) was used with a 25-gauge bipolar concentric needle, settings with amplitude of 50 to 100μV, 10- to 100-ms sweep speeds, and a grounding clamp at the exposed lateral sternocleidomastoid muscle. The EMG recording needle was inserted directly into the center of the defect/implant site, the adductor muscle complex, and the posterior cricoarytenoid muscle during laryngospasm and at rest. Immediately following electromyography, rats were humanely euthanized and tissue collected.

2.2.5 Histopathological and Histochemistry Assessment

After euthanasia, rat larynges with implanted engineered muscle were harvested en bloc, fixed in 4% paraformaldehyde overnight, and then transferred to 30% sucrose at 4°C for an additional 24 hours. Cryosections (25μm thickness) were prepared on a Thermo Cryotome FE (Fisher Scientific, Kalamazoo, MI). Sections were stained with hematoxylin & eosin (H&E) for histopathological analysis. Slides were viewed on a Nikon upright microscope (Eclipse E200, Nikon, Melville, NY) and images captured with a Leica camera (DFC480, Leica Buffalo Groove, IL).

For histochemistry analysis, all specimens were washed with phosphate buffered saline (PBS) 3 times, permeabilized with 0.1% Triton X-100 for 20 minutes, and blocked with 1% bovine serum albumin for 2 hours. Whole engineered muscle constructs were incubated overnight at 4°C with Alexa Fluor 488 conjugated phalloidin (1:25 Molecular Probes, Eugene, OR) for visualization of F-actin and counterstained with Draq5 (1:1000 Cell Signaling, Danvers, MA 4084L) nuclear stain. For staining tissue explant cryosections, beta III tubulin conjugated primary antibody (1:10 NL647 Molecular Probes) was applied and incubated overnight at 4°C. After rinsing extensively, slides were incubated with Alexa Fluor 594 conjugated α-bungarotoxin (1:100) for 2 hours at room temperature. Slides were rinsed and mounted with Fluorogel for imaging on an Olympus Fluoview confocal microscope (IX81, Olympus Waltham, MA).

2.3 Results

2.3.1 Flow-Aligned Cell-Oligomer Constructs Prepared With High Cell Density and Low Collagen-Fibril Density Support Enhanced Myotube Formation *In Vitro*.

A challenge associated with tissue-engineered muscle is the rapid and reproducible fabrication of muscle constructs with uniform cell alignment and physiologically-relevant ECM associations. Here, polymerization of C2C12-oligomer solutions in flow resulted in constructs with both component collagen-fibrils and myoblasts aligned in the direction of flow (Figure 2.1A-C). In contrast, when conventional casting techniques were applied, cells were uniformly distributed within a randomly organized collagen-fibril matrix (Figure 2.1D-F). The flow-

alignment method was then applied to determine the optimal cell and collagen-fibril density (stiffness) to achieve myotube formation.

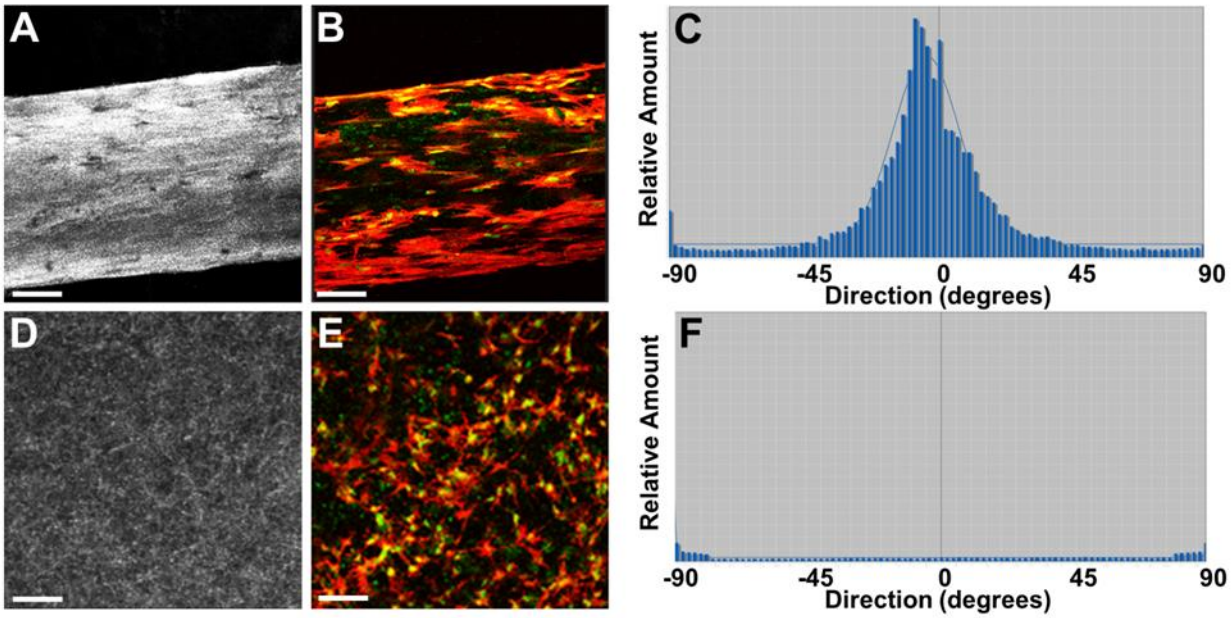

Figure 2.1. Representative images and directionality analyses for engineered muscle constructs created using flow alignment method (A–C) compared to conventional monodispersion technique (D–F). Fabricated muscle constructs were cultured 24 hours and analyzed by confocal reflection microscopy for visualization of fibril microstructure (A, D), confocal fluorescence microscopy for visualization of myoblast morphology (B, E; green =actin; blue=nuclei), and ImageJ Directionality algorithm for alignment determination (C, F). Scale bar = 50μm.

As indicated in Figure 2.2, constructs prepared at high cell density and low collagen-fibril density exhibited the necessary cell-cell interactions and matrix support to facilitate cell fusion and nuclear alignment.

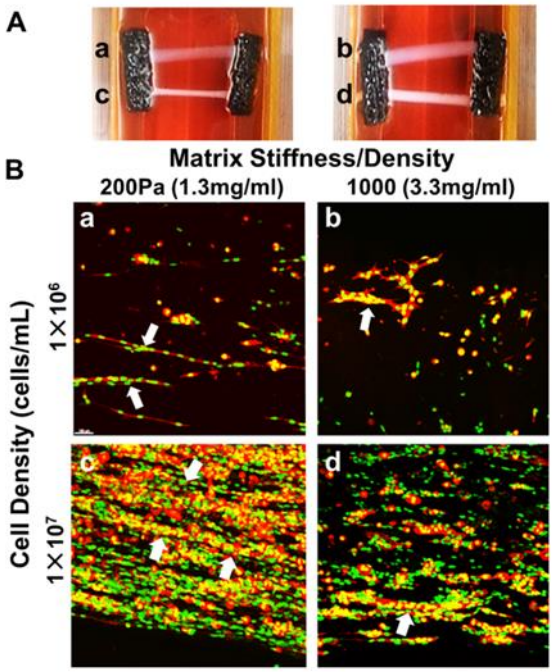

Figure 2.2. Tissue-engineered muscle construct culture and optimization. Muscle constructs were created by flow alignment of C2C12 myoblasts at 10E6 cells/mL (a, b) or 10E7 cells/mL (c, d) within type I collagen oligomer matrices prepared at 200 Pa (a, c) and 1,000 Pa (b, d). (A) Constructs were cultured within a custom culture device for 14 days under passive tension. (B) Confocal images (100 µm thickness) of 14-day constructs stained with phalloidin (F-actin; red) and Draq5 (nucleus, green) show more extensive myotube formation (white arrows) for constructs prepared at high cell densities (10E7 cells/mL) within low stiffness matrices (200 Pa). Scale bar=50 µm. Pa=pascal.

Follow-up verification studies revealed that this fabrication strategy was also applicable to primary rat MPCs, yielding highly reproducible engineered muscle with viable cells distributed throughout the construct after 2 weeks of culture (Figure 2.3).

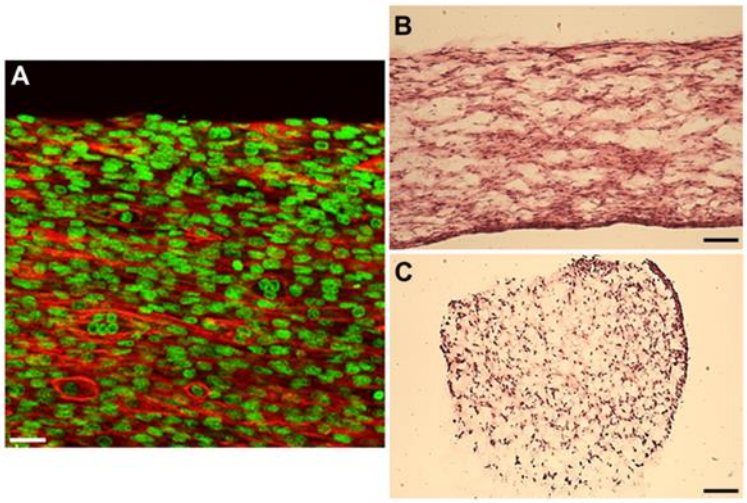

Figure 2.3. Engineered muscle constructs (14 days) prepared via flow alignment of F344 primary MPC (10E7 cells/mL) and 200 Pa oligomer collagen. (A) Confocal images (50 mm thickness) of 14-day constructs stained with phalloidin (F actin, red) and Draq5 (nucleus, green) show highly aligned cell morphology and fused myotube formation. Cells were distributed throughout the entire construct volume as indicated by H&E staining of longitudinal (B) and transverse (C) sections. Scale bars=30 μm (A), 500 μm (B–C). H&E=hematoxylin & eosin; Pa=pascal.

2.3.2 Reconstruction of Laryngeal Defects With MPC-Oligomer Constructs Yields Myogenesis, Neurovascular Regeneration, and Tissue Integration in Absence of Inflammatory-Mediated Foreign Body Response.

During the post-surgical period, all animals steadily gained weight and showed no signs of laryngeal compromise. As expected, partial laryngectomy with resection of cartilage and muscle and no treatment resulted in a healing response marked by inflammation and fibrous tissue formation within the defect area (Figure 2.4A). In contrast, oligomer implants, with and without MPCs, showed no significant inflammatory reaction and integrated rapidly with adjacent host tissues (Figure 2.4B-D). A surprising finding was that chondrogenesis accompanied muscle regeneration over time (Figure 2.4D). Compared to the oligomer-only group, MPC-oligomer and MEE-oligomer constructs showed more rapid muscle regeneration and maturation as evidenced by obvious striations within the implants as early as 1 month that became more evident at 3 months.

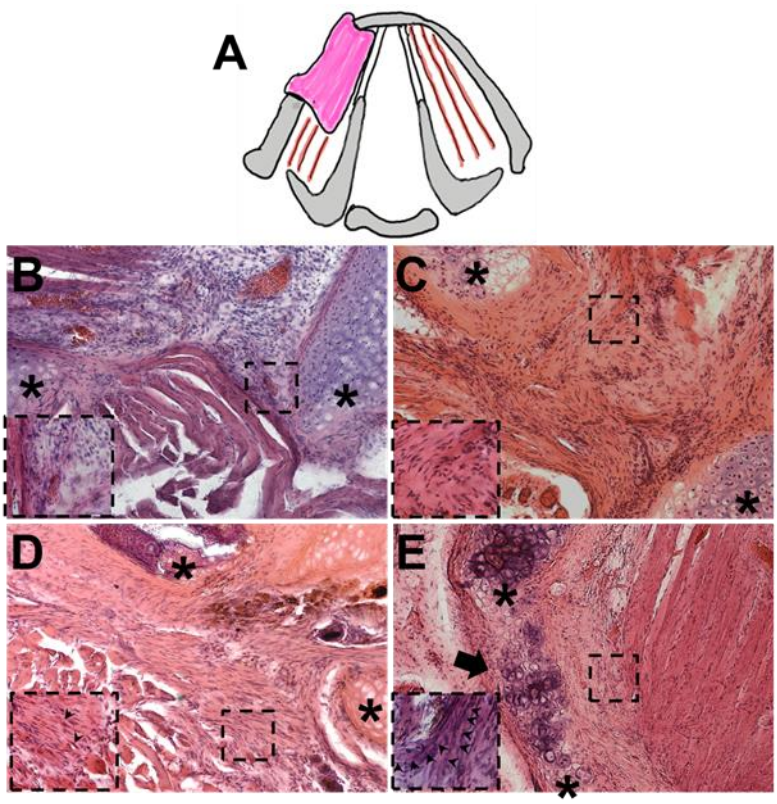

Figure 2.4. (A) Schematic showing partial laryngectomy model, which involved removal of a section of hemi-thyroid cartilage and associated underlying adductor muscle from the left side. Cross-section of rat larynx showing surgical procedure and implant placement. (B–E) Representative H&E stained sections of untreated control defect (B, 2 months) and defects treated with oligomer-only implant (C, 2 months), engineered muscle implant (D, 1 month), and engineered muscle implant (E, 3 months). Untreated defect (A) showed gap filled with native sternohyoid muscle and healing via inflammation. Oligomer-only group showed no significant inflammatory response and construct populated with mesenchymal cells. Engineered muscle implants showed progressive increase in volume of striated muscle (arrows) and cartilage regeneration over time with similar responses observed for both MPC- and MEE-oligomer implants). Asterisk (*) indicate edges of cartilage defect. Inserts represent high magnification of boxed areas. Scale bar=200 mm. H&E=hematoxylin & eosin; MEE=motor endplate expressing; MPC=muscle progenitor cell. Pa=pascal.

By 3 months, the relative extent of striated muscle increased, and was supported by neurogenesis, as evidenced by prominent beta III tubulin staining arising from the graft-host tissue interface (Figure 2.5). Interestingly, results based on beta III tubulin and α-bungarotoxin staining indicated that the greatest level of innervation was achieved with the MEE-oligomer group.

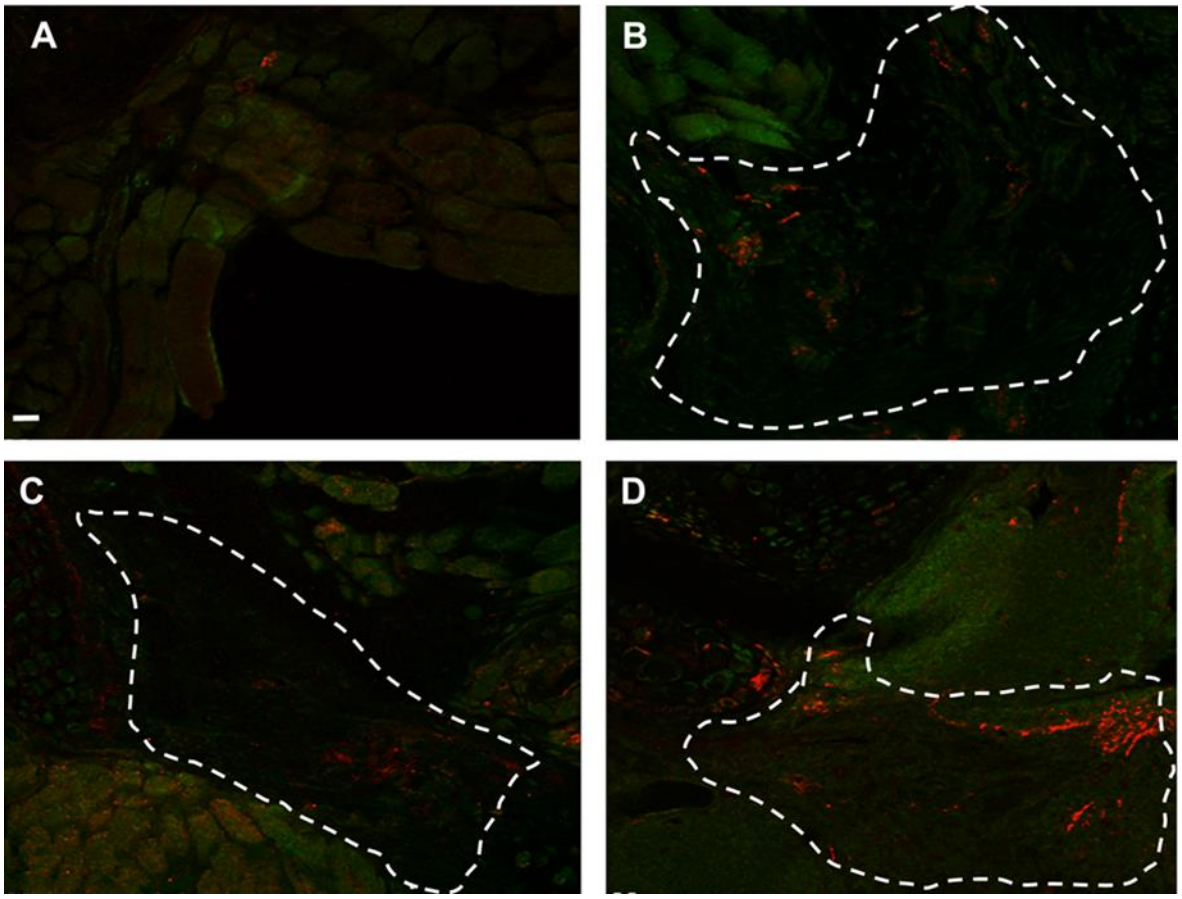

Figure 2.5. Beta III tubulin (red) and alpha bungarotoxin staining. (A) Defect-only control. (B) Collagen only control. (C) MPC implant at 3 month postop. (D) MEE implant at 3 month postop. The MEE-oligomer construct (D) has increased innervation when compared to the MPC oligomer construct (C). Both the MEE- and MPC-oligomer constructs have increased innervation when compared to the oligomer-only and untreated controls. Dotted line outlines approximate construct boundaries. Scale bar=100 mm. MEE=motor endplate expressing; MPC=muscle progenitor cell; postop=postoperative.

Qualitative EMG measurements provided further corroborating evidence of enhanced innervation of the MEE-oligomer constructs, with the MEE-oligomer group demonstrating the greatest level of motor unit activity (recruitment) during laryngospasm (Figure 2.6).

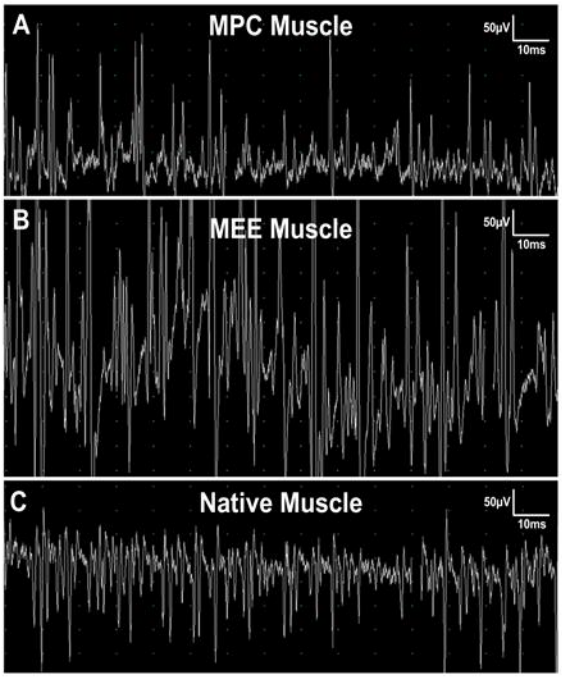

Figure 2.6. Representative electromyography tracings captured at 50 mV amplitude and 10 ms sweep speeds during active laryngospasm to detect firing within engineered muscle implant 3 months following implantation (A, B) or native adductor muscle complex (C). (A) Defect treated with engineered muscle prepared with muscle progenitor cells (MPC muscle) generated abundant, variable sized motor unit potentials. (B) Engineered muscle prepared with motor endplate expressing MPC (MEE muscle) generated potentials that were significantly larger in amplitude and frequency compared to MPC muscle and native adductor muscle. (C) Native adductor muscle complex demonstrated bursts of motor unit potentials during laryngospasm. MEE=motor endplate expressing; MPC=muscle progenitor cell.

2.4 Discussion

We and others have shown that significant muscular injuries result in a reparative inflammatory-mediated healing response yielding fibrotic scar and dysfunctional muscle. Here, the myogenic potential of MPCs was interfaced with a standardized self-assembling type I collagen-fibril matrix to create a 3D tissue-engineered muscle for laryngeal reconstruction. Flow-alignment and an optimized MPC-collagen-fibril density ratio were used to achieve cell-matrix physical and biochemical associations that mimicked those found between muscle cells and the endomysium *in vivo*, resulting in accelerated in-vitro myotube formation. Additional benefit of recapitulating the muscle-ECM interface was evident from the time-dependent recovery of muscle volume and function along with regeneration of supporting cartilaginous structures following implantation *in vivo*.

Results of these studies suggest that aligned MEE-oligomer constructs contributed to rapid tissue integration and regeneration in the absence of any significant inflammatory reaction,

yielding engineered muscle with enhanced innervation on histology, and functional elicitation of motor unit potentials. Major advantages of the model include the use of autologous cells strategically aligned, robust muscle neovascularization/innervation/survival, and a scalable model which could be translated into patient-specific designs. While the current study allowed a variety of constructs to be tested in vivo, the major limitation of such a rodent model is the small anatomic size and physiologic differences (lack of cough) preventing complete transmural hemilaryngectomies from being safely performed. Thus, animal studies with engineered muscle and cartilage will be needed in the future to better assess the full potential of the engineered muscle to recapitulate laryngeal structure and function.

2.5 Conclusion

Collectively, this work represents initial design optimization of a 3D tissue-engineered muscle implant prepared from therapeutic MPCs and type I collagen oligomers. This strategy overcomes a number of significant challenges related to skeletal muscle engineering including 1) the use of a standardized and customizable self-assembling collagen formulation, 2) promotion of interfacial tissue regeneration by minimizing inflammation and 3) acceleration of functional muscle recovery through rapid reinnervation in MEE constructs. While our current study suggests that MEE constructs receive robust innervation after implantation, further studies are needed to determine if these findings will translate into improved muscle contractility/function. Thus, these experiments represent initial steps towards the successful design and application of engineered autologous muscle implants for laryngeal repair and reconstruction.

2.6 Acknowledgements

These projects were supported in part by award number R01DC014070-01A1 from the National Institute on Deafness and Other Communication Disorders (NIDCD) within the National Institutes of Health (NIH). The content of this publication is solely the responsibility of the authors and does not necessarily represent the official views of the NIDCD or NIH. The authors would like to thank Alexis Zobel (2015 Summer Research Fellow) for her assistance with flow alignment method, Melissa Bible and the rest of the Weldon School of Biomedical

Engineering animal technical staff for their animal study support, and finally Will Hoggatt and Richard Brookes for the design and fabrication of the Ultem mold and custom culture device.

2.7 References

1. Howlader N, Noone AM, Krapcho M, Miller D, Bishop K, Altekruse SF, Kosary CL, Yu M, Ruhl J, Tatalovich Z, Mariotto A, Lewis DR, Chen HS, Feuer EJ, Cronin KA (eds). SEER Cancer Statistics Review, 1975-2013, National Cancer Institute. Bethesda, MD, http://seer.cancer.gov/csr/1975_2013/, based on November 2015 SEER data submission, posted to the SEER web site, April 2016.
2. Bian W, Bursac N. Tissue engineering of functional skeletal muscle: challenges and recent advances. IEEE Eng Med Biol Mag 2008; 27:109-113.
3. Mertens JP, Sugg KB, Lee JD, Larkin LM. Engineering muscle constructs for the creation of functional engineered musculoskeletal tissue. Regen Med 2014; 9:89-100.
4. Gillies AR, Lieber RL. Structure and function of the skeletal muscle extracellular matrix. Muscle Nerve 2011; 44:318-331.
5. Cheng CS, Davis BN, Madden L, Bursac N, Truskey GA. Physiology and metabolism of tissue-engineered skeletal muscle. Exp Biol Med (Maywood) 2014; 239:1203-1214.
6. Ostrovidov S, Hosseini V, Ahadian Set al. Skeletal muscle tissue engineering: methods to form skeletal myotubes and their applications. Tissue Eng Part B Rev 2014; 20:403-436.
7. Halum SL, Bijangi-Vishehsaraei K, Zhang H, Sowinski J, Bottino MC. Stem cell-derived tissue-engineered constructs for hemilaryngeal reconstruction. Ann Otol Rhinol Laryngol 2014; 123:124-134.
8. Morehead JM, Holt GR. Soft-tissue response to synthetic biomaterials. Otolaryngol Clin North Am 1994; 27:195-201.
9. Porzionato A, Sfriso MM, Pontini Aet al. Decellularized Human Skeletal Muscle as Biologic Scaffold for Reconstructive Surgery. Int J Mol Sci 2015; 16:14808-14831.
10. Hinds S, Bian W, Dennis RG, Bursac N. The role of extracellular matrix composition in structure and function of bioengineered skeletal muscle. Biomaterials 2011; 32:3575-3583.

11. Rhim C, Lowell DA, Reedy MCet al. Morphology and ultrastructure of differentiating three-dimensional mammalian skeletal muscle in a collagen gel. Muscle Nerve 2007; 36:71-80.
12. Rossi CA, Pozzobon M, Ditadi Aet al. Clonal characterization of rat muscle satellite cells: proliferation, metabolism and differentiation define an intrinsic heterogeneity. PLoS One 2010; 5:e8523.
13. Huang YC, Dennis RG, Larkin L, Baar K. Rapid formation of functional muscle in vitro using fibrin gels. J Appl Physiol (1985) 2005; 98:706-713.
14. Powell CA, Smiley BL, Mills J, Vandenburgh HH. Mechanical stimulation improves tissue-engineered human skeletal muscle. Am J Physiol Cell Physiol 2002; 283:C1557-1565.
15. Kreger ST, Bell BJ, Bailey Jet al. Polymerization and matrix physical properties as important design considerations for soluble collagen formulations. Biopolymers 2010; 93:690-707.
16. Bailey JL, Critser PJ, Whittington C, Kuske JL, Yoder MC, Voytik-Harbin SL. Collagen oligomers modulate physical and biological properties of three-dimensional self-assembled matrices. Biopolymers 2011; 95:77-93.
17. Blum KM, Novak T, Watkins L, Neu CP, Wallace JM, Bart ZR, Voytik-Harbin SL. Acellular and cellular high-density, collagen-fibril constructs with suprafibrillar organization. Biomater Sci 2016; 4:711-723.
18. Voytik-Harbin SL, Han B. Collagen-cell interactions and modeling in microenvironments. In: Neu CP, Genin G, eds. CRC Handbook of Imaging in Biological Mechanics. Boca Raton, Florida: Taylor & Francis Group; 2015:261-273.
19. Whittington CF, Yoder MC, Voytik-Harbin SL. Collagen-polymer guidance of vessel network formation and stabilization by endothelial colony forming cells in vitro. Macromol Biosci 2013; 13:1135-1149.
20. Critser PJ, Kreger ST, Voytik-Harbin SL, Yoder MC. Collagen matrix physical properties modulate endothelial colony forming cell-derived vessels in vivo. Microvasc Res 2010; 80:23-30.

21. Yrineo AA, Adelsperger AR, Durkes ACet al. Murine ultrasound-guided transabdominal para-aortic injections of self-assembling type I collagen oligomers. J Control Release 2017; 249:53-62.
22. ASTM Standard F3089: Characterization and Standardization of Polymerizable Collagen-Based Products and Associated Collagen–Cell Interactions; ASTM International: West Conshohocken, PA, 2014; DOI: 10.1520/F3089-14; www.astm.org.

CHAPTER 3. MOTOR ENDPLATE-EXPRESSING CARTILAGE-MUSCLE IMPLANTS FOR RECONSTRUCTION OF A DENERVATED HEMILARYNX

Chapter 3 represents an article published in The Laryngoscope 129 (6), 1293-1300, 2019

3.1 Introduction

Laryngeal cancer is one of the most commonly diagnosed airway cancers, with over 13 thousand new cases diagnosed annually in the United States alone[1]. Standard treatments for advanced cancer, which involve surgical resection and/or chemoradiation, are life-saving but may render patients dependent on a tracheostomy and/or feeding tube with poor quality of life. A recent review by Hamilton and Birchall indicated that one treatment strategy for advanced laryngeal cancer is to tissue engineer a functional laryngeal replacement.[2] This, they postulate, can be broken down into a number of design considerations including restoration of i) structure through scaffold design and ii) function by promoting skeletal muscle regeneration with associated vascularization and innervation. Autologous grafts, such as myocutaneous flaps and buccal mucosa, can be too bulky and come with donor site availability and morbidity problems. Approaches aimed at recapitulating laryngeal structure have included using decellularized larynx[3], decellularized cartilage[4], or various natural and synthetic biomaterials seeded with cells[5-10]. Major limitations of these approaches have been inadequate integration with the surrounding host tissue, significant inflammatory response, and poor vascularization/tissue survival. Another vital component to engineering a functional larynx is to restore nerve and muscle function. Since laryngectomy surgery is often associated with injury of the recurrent laryngeal nerve (RLN), it is important to include denervation in the preclinical animal model. Halum[11] and Paniello[12] have shown that use of muscle progenitor cells (MPCs) induced to express motor endplates improves reinnervation and function post RLN injury.

To begin to address these challenges, our group has previously shown that we can replace thyroid cartilage with a novel oligomeric collagen-adipose stem cell implant[16] that enhances cartilage healing with no inflammatory foreign body reaction. We have also shown that replacement of resected adductor muscle complex with a tissue-engineered (TE) skeletal muscle

implant not only is well tolerated by the animal, similar to the cartilage implant, but that it also improves function (on EMG) when compared to controls[11]. We now extend this work by investigating the integrated use of TE muscle-cartilage implants for reconstruction of partial laryngectomy defects in the presence and absence of RLN injury in a rodent model. This preclinical model was designed to recreate the clinically-relevant surgical reconstruction scenario where neoplastic resection is performed with RLN injury. The purpose of this study was to examine the microscopic, structural, and functional outcomes of TE muscle-cartilage implants for repair of a denervated hemilarynx after partial laryngectomy (resection of outer cartilage/adductor muscle).

3.2 Materials and Methods

3.2.1 Primary Muscle Progenitor Cell Isolation and Culture

Primary MPCs were generated from skeletal muscle biopsies obtained from 12-week-old male Fischer 344 rats (Envigo, Indianapolis, IN) as previously described.[11] Briefly, fresh muscle tissue was minced in myogenic growth medium (MGM; DMEM, 1% PSF-1, 20% fetal bovine serum, and 0.1% chick embryo extract (Accurate Chemicals, Westbury, NY)) and digested in 0.2% collagenase type I (EMD Millipore, Temecula, CA) at 37°C for 2 hours. Digested tissue was filtered through a 100μm cell strainer, plated onto untreated 100mm petri dishes (Fisher Scientific), and cultured overnight at 37°C with 5% CO_2. The supernatant was removed the next morning and transferred to culture flasks (Corning Life Sciences, Corning, NY). Cells were cultured to 70% confluency and used in experiments at passages 3 to 5.

3.2.2 Fabrication of Engineered Skeletal Muscle Constructs

Muscle implants were fabricated as previously described.[11] Briefly, MPC's from F344 rats were suspended in type I oligomeric collagen (2.0 mg/mL) and flowed through a 4mm cylindrical mold. Once polymerized, implants were cultured under passive tension in DMEM supplemented with 1% PSF-1, and 10% FBS at 37°C and 5% CO_2 for 5 days, with medium changes every 2 days. On day 5, medium was changed to differentiation medium, representing DMEM supplemented with 8% horse serum (HyClone) and 1% PSF-1, and constructs were cultured for an additional 7 days to induce myotube formation.

For a subset of experiments, MPCs were induced to express motor endplates (MEE) as described previously.[15] Briefly, muscle constructs were allowed to differentiate for 5 days at which point acetylcholine chloride (40 nM; Tocris Bioscience, Bristol, England), agrin (10 nM; R&D Systems, Minneapolis, Minnesota), and neuregulin (2 nM; R&D Systems) were added to the medium. Constructs were cultured an additional 7 days with medium changes every 3 days. Motor endplate expression was confirmed by immunostaining with Alexa Fluor 594 conjugated α-bungarotoxin (Molecular Probes, Eugene, Oregon).

3.2.3 Fabrication of Engineered Cartilage Constructs

Cartilage constructs were fabricated as previously described.[16] Briefly, F344 rat ASCs were suspended in type I oligomeric collagen (4.0 mg/ml) and polymerized. They were then compressed to 0.5-mm-thick constructs (75 mg/ml) and cultured in chondrogenic differentiation medium (Hyclone Advance Stem Chondrogenic Differentiation Medium, SH30889.02; Thermo Scientific, Waltham,MA) and were maintained in a 37^{o}C, 5% CO_2 incubator for up to 4 weeks. The medium was changed twice per week.

3.2.4 Laryngectomy, Recurrent Laryngeal Nerve Injury and Implantation of Engineered Muscle

Engineered muscle constructs were implanted in our established rat partial laryngectomy model.[15] The animal study protocol was approved by Purdue Animal Care and Use Committee, and institutional guidelines, in accordance with the National Institutes of Health, were followed for the handling and care of the animals. In brief, twelve Fisher 344 rats were anesthetized with intraperitoneal injection of xylazine and ketamine and then maintained on 1% to 4% isoflurane. The ventral larynx was exposed via a midline incision. The sternohyoid muscle was incised and reflected to expose the thyroid cartilage. A section (approximately 2mm x 2mm) of thyroid cartilage and associated adductor muscle was removed from the left side. Animals were randomized into groups receiving implants made with MPC or MEE cells with and without RLN injury. All groups received identical cartilage implants with endpoints at 1, 3, and 6 months. The muscle construct was placed into the defect (similar to a medialization laryngoplasty implant), followed by the cartilage construct over top (Figure 1) with extrusion prevented by suturing overlying sternohyoid muscles over the cartilaginous defect. For groups with RLN injury, the left

recurrent laryngeal nerve was cauterized as it entered the larynx. The subcutaneous tissue and skin were then closed with 5-0 Vicryl suture.

3.2.5 Video Laryngoscopy and Laryngeal Electromyography (EMG)

At 1, 3, and 6 month endpoints, video laryngoscopy and laryngeal electromyography were performed under isoflurane anesthesia as previously described.[11] Video laryngoscopy was performed using a rigid endoscope with attached camera. Electromyogram (EMG) recordings (Niking Viking Quest electromyography machine, Madison, Wisconsin) were collected with a 25-gauge bipolar concentric needle, 50 to 100μV amplitude, 10- to 100-ms sweep speeds, and a grounding clamp at the exposed lateral sternocleidomastoid muscle. The EMG recording needle was inserted directly into the center of the defect/implant site, the adductor muscle complex, and the posterior cricoarytenoid muscle during laryngospasm (produced via lightening the isoflurane anesthesia and stimulating with needle) and at rest. Immediately following electromyography, rats were humanely euthanized and tissue collected.

3.2.6 Histopathological and Histochemistry Assessment

After euthanasia, rat larynges and associated implants were harvested en bloc, fixed in 4% paraformaldehyde overnight, and then transferred to 30% sucrose at 4^{o}C for an additional 24 hours. Cryosections (25μm thickness) were prepared on a Thermo Cryotome FE (Fisher Scientific, Kalamazoo, MI). Sections were stained with hematoxylin & eosin (H&E) and Alcian blue for histopathological analysis. Slides were viewed on a Nikon microscope (Eclipse E200, Nikon, Melville, NY) and images captured with a Leica camera (DFC480, Leica Buffalo Groove, IL). As previously described, myofiber diameter was evaluated by measuring the lesser fiber diameter using Image J software (NIH, Bethesda, MD).[17]

For histochemistry analysis, all specimens were washed with phosphate buffered saline (PBS) 3 times, permeabilized with 0.1% Triton X-100 for 20 minutes, and blocked with 1% BSA for 2 hours. For staining tissue explant cryosections, beta III tubulin conjugated primary antibody (1:10 NL555 Molecular Probes) was applied and incubated overnight at 4^{o}C. After rinsing extensively, slides were incubated with Alexa Fluor 488 (Molecular Probes) conjugated α-bungarotoxin (1:100) for 2 hours at room temperature. Slides were rinsed and mounted

with Fluoro-Gel (Electron Microscopy Sciences, Hatfield, PA) for imaging on a Zeiss LSM 880 confocal microscope (Oberkochen, Germany). The number of motor endplates with nerve contact were counted and divided by the total number motor endplates to give percent innervation, as previously described.[11]

3.2.7 RNA isolation and RT and qPCR:

Total RNA was extracted using the TRIzol method. The cDNA was synthesized using 100μg of RNA and random hexamers in SuperScript-III kit (Invitrogen, Carlsbad, CA) according to manufacturer recommendations. The resulting cDNA was then amplified by PCR using Go Taq DNA Polymerase system (Pronega, Madison, WI). Primers used are listed in Table 1. A single cycle consisted of 15-second denaturation at 94°C, 30-second annealing at 55°C, and 60-second extension at 72°C. 38 cycles were used for GAPDH, NTN-1, and NT-4, 35 cycles were used for NT-3 and GDNF. A 10ul sample of reaction mixture was electrophoresed in a 2% agarose gel containing ethidium bromide to evaluate the amplification and determine the size of the generated fragments. A 100 bp DNA ladder was used as a standard size marker. Densitometry was performed for relative band quantification. Intensity was measured using Image J software (NIH) and results normalized to GAPDH.

Table 3.1. PCR primer sequence

Primer name	Forward (5'-3')	Reverse(5'-3')
NTN-1	CTTCATGTTCATCTTCAGTTTTCCT	CTTGCATTAAGATTCCTGTAGCG
NT-3	ACATCACCTTGTTCACCTGTA	GTTCCACCTTTCTCTTCATGTC
NT-4	CCCTGCGTCAGTACTTCTTCGAGAC	CTGGACGTCAGGCACGGCCTGTTC
GDNF	GGTCTACGGAGACCGGATCCGAGGTGC	AGATAAACAAGCGGCGGCAC
GAPDH	GGTCTACGGAGACCGGATCCGAGGTGC	AACTCCCTCAAGATTGTCAGCA

3.2.8 Statistical Analysis

Student t test was used for all analysis and $p<0.05$ was considered significant.

3.3 Results

3.3.1 Muscle and Cartilage Implant Integration

All animals survived the post-surgical period with no life-threatening complications. Some RLN injured animals showed mild stridor but this resolved with time. All animals steadily gained weight over the study period. Post-mortem gross pathological exam showed integration of the cartilage and muscle implants into host tissue with no macroscopic signs of inflammation. Alcian blue staining of cryo-sectioned specimens was weakly positive at 1 month (Figure 3.1B). At 3 and 6 month timepoints, sections demonstrated darker blue staining consistent with glycosaminoglycan deposition and cartilage formation (Figure 3.1 C-D). H&E staining at 1 month displayed immature muscle neighboring native adductor muscle with no foreign body inflammatory response (Figure 3.2A). At 3 months, maturation of the muscle within the implant was demonstrated by development of cross striations and myofiber alignment (Figure 3.2B). By 6 months, little to no immature muscle was visible within the defect area suggesting complete integration with native tissue (Figure 3.2C).

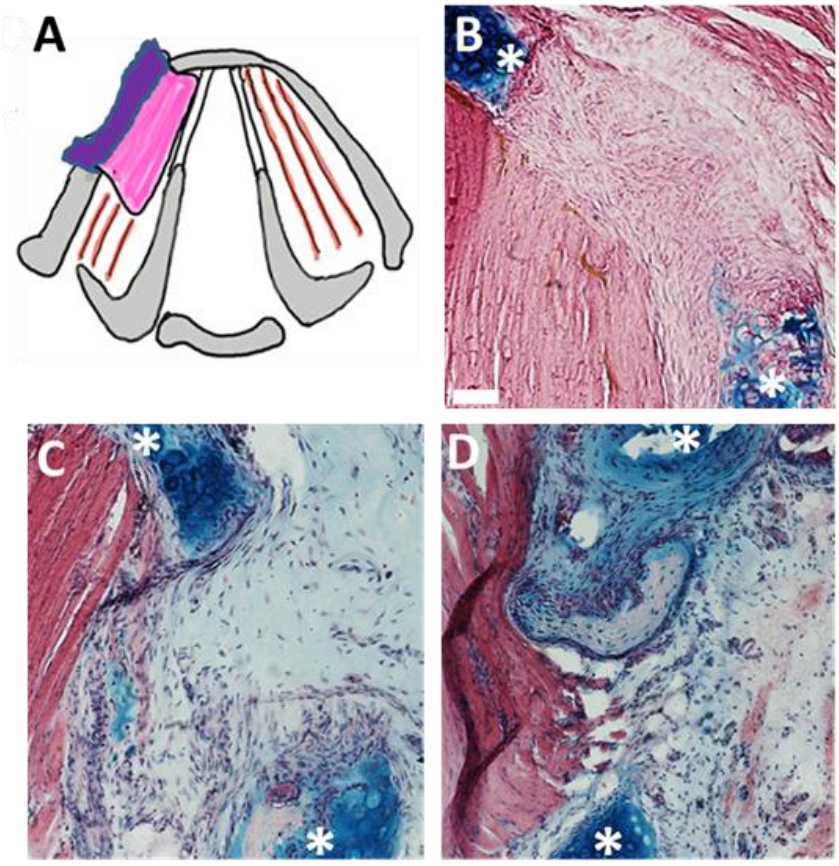

Figure 3.1. (A) Schematic diagram of surgical procedure. Alcian blue staining shows progressive healing and differentiation of the cartilage construct over the 1-month (B), 3-month (C), and 6-month (D) timepoints. Increase in blue staining indicates progressive cartilage regeneration, proteoglycan deposition, and maturation. *= Edges of surgically created defect. Scale bar = 100 μm.

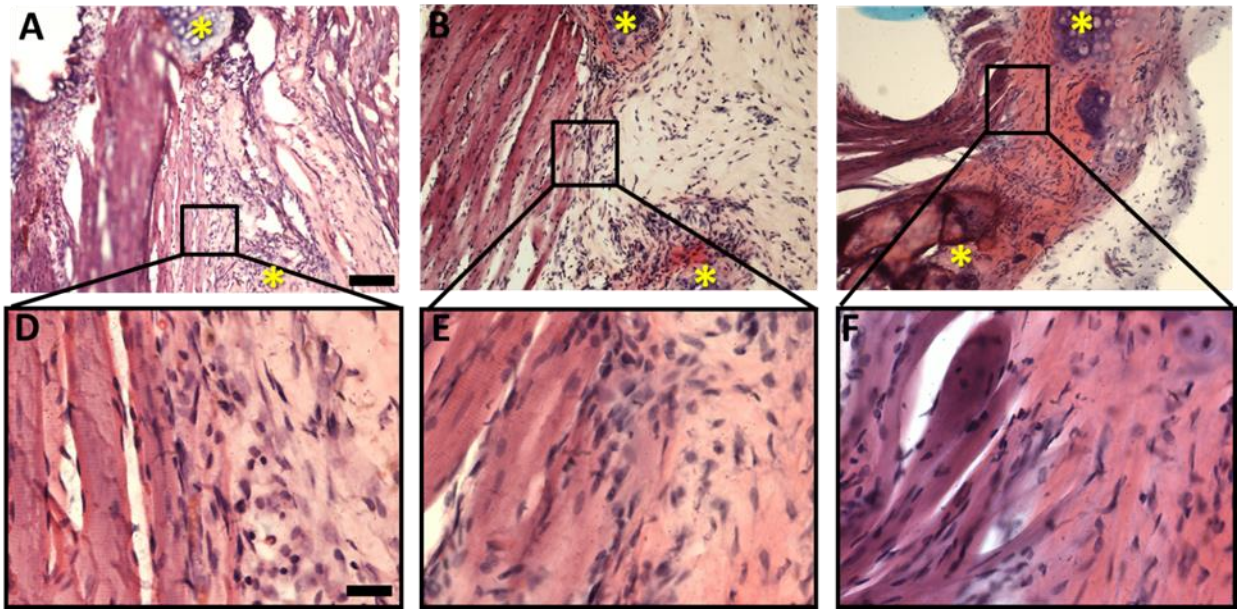

Figure 3.2: H&E staining shows progressive healing of surgical defect at 1 month (A,D), 3 months (B,E), and 6 months (C,F), marked by muscular integration and regeneration with no inflammatory response. Asterix marks edges of surgical defect. Scale Bar: A-C 100μm; D-F 25μm

3.3.2 Muscle Implant Functional Results after RLN Injury

α-bungarotoxin and beta III tubulin staining demonstrated that implants that were induced to form motor endplates (MEE) showed a greater number of motor endplates and robust innervation (Figure 3.3). Further, both the TA and PCA muscles showed significantly increased motor endplate to nerve contact in the MEE treated group ($p<0.01$ Figure 3.4).

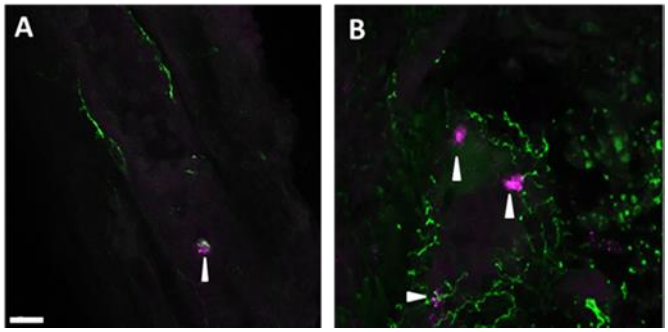

Figure 3.3. α-bungarotoxin (pink) and beta III tubulin (green) staining shows presence of motor endplates and significant innervation of the engineered muscle implants after 6 months. (A) MPC implants showed a lesser degree of innervation. (B) Motor endplate-expressing implants showing robust innervation and motor endplates (arrowheads). Scale bar: 10 μm.

Further, both the TA and PCA muscles showed increased motor endplate to nerve contact in the MEE treated group (Figure 3.4).

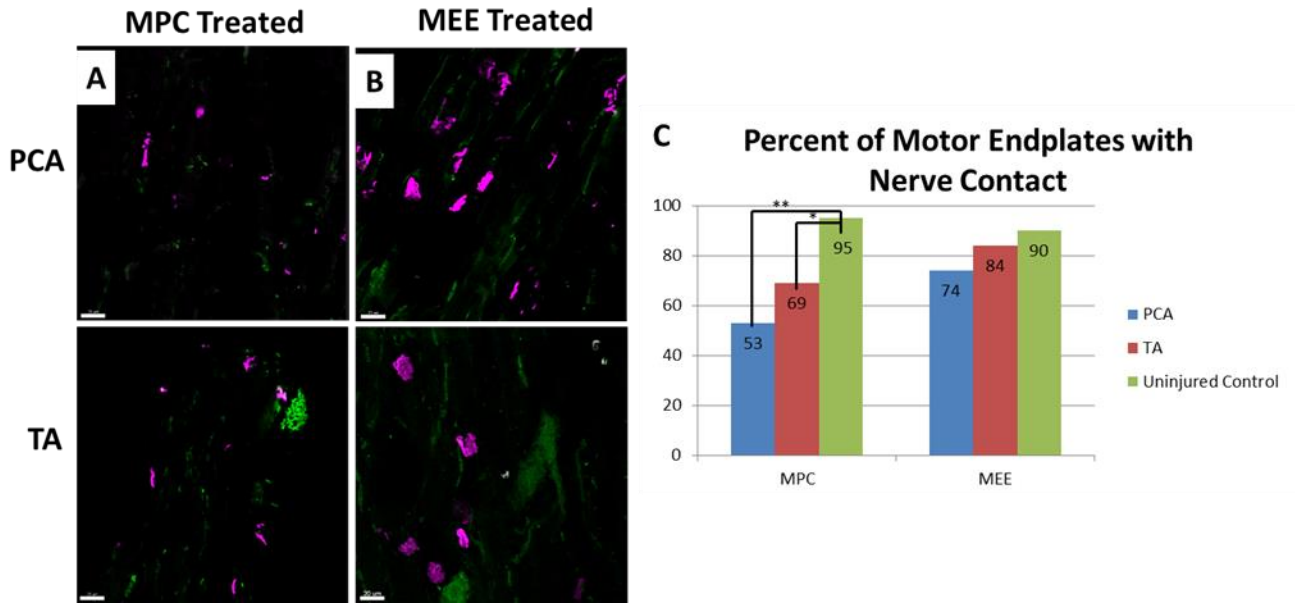

Figure 3.4. MEE implants induce an increased percentage of MEP compared to MPC implants, with nerve contact in abductor and adductor muscles. Motor endplate (α-bungarotoxin, pink) and nerve (beta III tubulin, green) staining of PCA and TA muscles in the MPC-treated (A) and MEE-treated (B) groups. The number of motor endplates with nerve contact were counted and divided by the total number of motor endplates to give percent innervation of each muscle compared to an uninjured control (C). *P < 0.05. **P < 0.01. Scale bar: 20 μm. MEE = motor endplate-expressing; MPC = muscle progenitor cells.

Qualitative EMG measurements of the adductor muscle complex of the MSC treated animals showed low level activity (Figure 3.5A) whereas the MEE treated animals showed near normal muscle activity, with interference and recruitment patterns (during laryngospasm) that mimicked normal adductor muscle (Figure 3.5C). This finding was further corroborated by adductor muscle complex myofiber diameter measurements, with values for MEE treated animals significantly greater than those for MSC treated animals ($p<0.001$ Figure 3.5E).

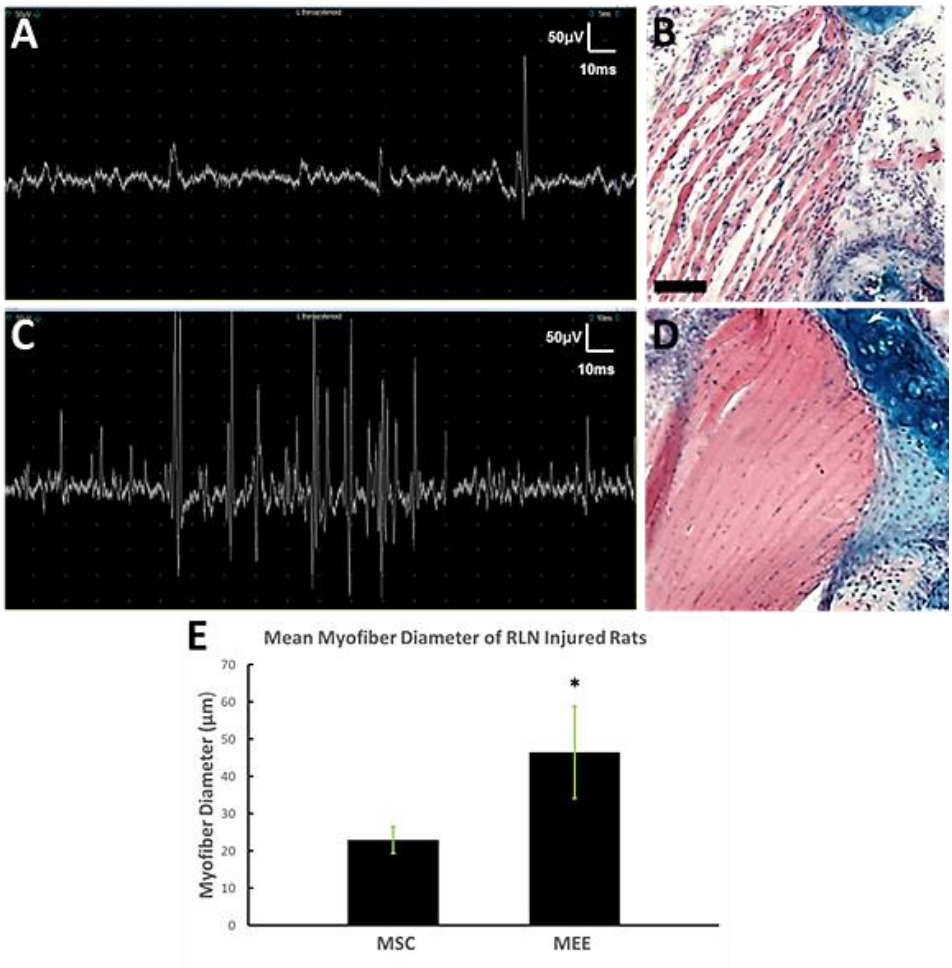

Figure 3.5: RLN-injured animals treated with MEE implants showed increased EMG activity and myofiber diameter compared to MSC implants. EMG of the adductor muscle complex showed increased activity in MEE-treated (C) animals compared to MSC-treated (A) animals. Histology showed myofiber atrophy and inflammatory cell infiltrate in MSC (B) animals and normal architecture in MEE (D) animals. (E) Myofiber diameter of adductor muscle showed significant increase in MEE-treated animals (Mean ± standard deviation, P <0.001, 2 animals per group, minimum 36 measurements per animal). Scale bar: 100µm EMG = electromyography; MEE = motor endplate-expressing; RLN = recurrent laryngeal nerve.

In nerve injured animals, video laryngoscopy showed function recovery in all animals receiving the MEE implant with definitive although slightly delayed movement at all timepoints of both adductor and abductor muscles. By contrast, none of the animals receiving the MSC implant showed definitive movement at any timepoint (Figure 3.6).

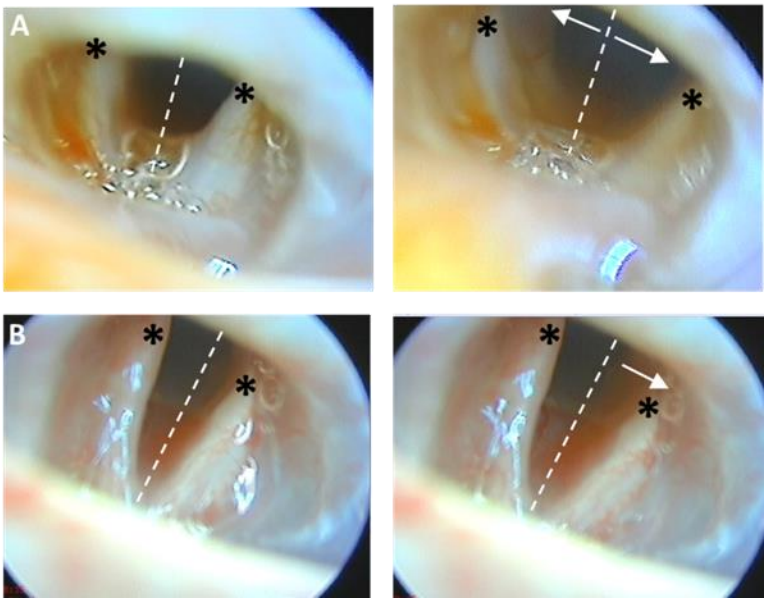

Figure 3.6: Still images from video laryngoscopy show recovery of left vocal fold movement in animals treated with motor endplate-expressing implants (A). Animals treated with the MPC implant (B) showed little to no movement in the left vocal fold at any time point.

3.3.3 PCR

Quantification of PCR expression based on band intensity revealed statistical differences between differentiated MPCs and MEEs (Figure 3.7). Specifically, significant differences ($p<0.05$) were detected between the MPC and MEE expression of NT-3, NTN-1, NT-4 and GDNF (2 versus 3, respectively). Thus, the MEE induction was associated with increased neurotrophic factor expression in all the factors tested.

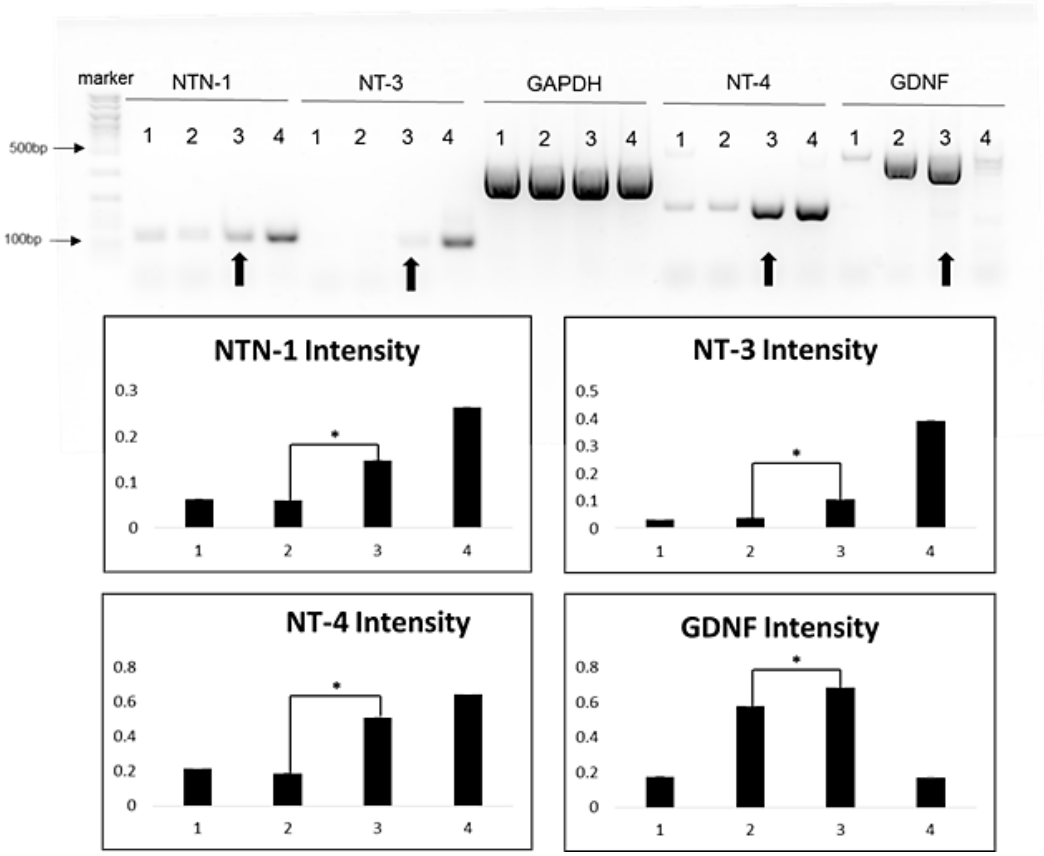

Figure 3.7: A, Reverse transcription polymerase chain reaction results show cells induced to express MEE have increased expression of neurotropic factors when compared to MPCs. 1: Undifferentiated MPC (negative control); 2: differentiated MPC; 3: MEE cells (arrows); and 4: brain (positive control). B, Band intensity measurements for each factor normalized to GAPDH. Statistics comparing MPC vs. MEE cells (*P < 0.01). MEE = motor endplate-expressing; MPC = muscle progenitor cells.

3.4 Discussion

We have previously demonstrated that aligned muscle implants[11] and cartilage implants[16] individually integrate with host tissue and differentiate with no foreign body reaction in a rat model of partial hemilaryngectomy. With the long-term goal of developing new therapeutic options for restoring or replacing damaged or diseased airway (larynx), we extended those studies with the first application of combined tissue engineered cartilage-muscle implants following partial hemilaryngectomy with and without RLN injury. Study results showed that the two-layer implant demonstrated viability and structural integrity comparable to the respective single layers. Such findings are important because this brings us closer to the ideal multi-layer functional tissue-engineered larynx for clinical applications. Of course, this study is limited in that it represents an early stage of investigation using a small animal model; potential clinical

applicability cannot be determined until functional survival is demonstrated in large animal models, followed by clinical trials.

Differentiating features inherent to our TE larynx design include the use of a 1) self-assembling type I oligomeric collagen for scaffold customization and cell encapsulation and 2) specialized muscle progenitor cells chemically-induced to express motor end plates. Scaffolds and tissue constructs fabricated with oligomeric collagen take advantage of collagen's inherent capacity for molecular self-assembly and natural intermolecular crosslinks which serve to physically stablize resulting fibril network and slow collagen turnover (resist proteolytic degradation).[18,19] As a result, the collagen-fibril scaffold, together with its resident cells, rapidly integrate with host tissue, such that both physical and biochemical cues (e.g., mechanical forces) inherent to the local tissue microenvironment can be effectively transmitted to guide cell phenotype and function. The significance of this mechanochemical signalling was evidenced by the progressive maturation of the muscle and cartilage implants in absence of a significant inflammatory reaction. By contrast, conventional biodegradable biomaterials and decellularized tissues are often not amenable to cell encapsulation and yield tissue responses characterized by inflammatory-mediated degradation and/or fibrotic capsule formation, which are known to delay or prevent tissue vascularization and regeneration.[20,21] Additionally, the no treatment controls, reported previously, showed scarring of the defect and a marked inflammatory response.[11]

Our TE construct incorporates MEE muscle cells with the goal of accelerating and guiding more organized neuromuscular junction formation[22]. Our previous study[11] with intact RLN showed enhanced innervation, based on motor endplate to nerve contact and electromyography (EMG) activity, of engineered muscle constructs when MEE muscle cells were used to create the implants. Similarly, Paniello[12] showed injection of MEE muscle cells in dogs with RLN injury resulted in increased innervation based on motor-endplate to nerve contact, which in turn contributed to increased muscle mass and measured laryngeal adductor pressure. Our current results suggest that animals receiving MEE constructs with complete RLN transection injury show increased laryngeal re-innervation (based on motor endplate to nerve contact and EMG) and qualitatively functional (based on video laryngoscopy) gains of both adductor and abductor muscle complexes when compared to animals treated with MPC implants. Notably, the presence of MEE implants attenuated atrophy of muscle, allowing for improved function post-injury. Our hypothesis is that the chemical signaling by the MEE cells

improves innervation and thus function post injury. Our RT-PCR data further supports this hypothesis showing that MEE cells have increased expression of multiple neurotropic factors (Figure 3.7).

While tissue-engineered implants are still clinically in their infancy, one advantage of an autologous cell-based implant is that no immunosuppression is required—potentially a major safety advantage, as the first laryngeal transplant done for laryngeal cancer resulted in rapid tumor recurrence and patient death due to the required immunosuppression[23]. Other advantages to the use of autologous stem cells include the promotion of tissue regeneration, promotion of angiogenesis, and inhibition of inflammation. Many of these effects are mediated via the release of a wide array of cytokines from the cells leading to an autocrine mediated acceptance/integration/revascularization of the implanted tissue[24]. These same effects do raise safety concerns about using the implants in an oncologic setting. However, investigations suggest cells such as adipose stem cells have antineoplastic effects with malignancies such as pancreatic adenocarcinoma, hepatocarcinoma, colon, and prostate cancers, and there are no reports of tumorigenesis in comparable tissue-engineered tissue, so we anticipate that oncologic safety will not be a major hurdle if appropriate surgical margins are attained at the time of initial resection. [25,26]

While we anticipated possible restoration of adductor function after reconstruction with the tissue-engineered implants, the finding of restored abduction and adduction in the MEE implants was an unexpected and exciting finding. Histology (percentage of motor endplates with nerve contact) supported strong reinnervation of both the PCA and adductor complex in the MEE implanted animals after RLN injury, although the PCA consistently had a greater percentage of motor endplates with nerve contact, likely suggesting earlier reinnervation due to the closer anatomic proximity of the PCA to regenerating RLN. This concept of obviating synkinesis by enhancing the speed of axonal regeneration was originally described with nimodipine therapy by Mattsson and colleagues,[27] and has been further supported with clinical investigations by Rosen and colleagues.[28,29] Thus, we hypothesize that the cytokine effects (expression of trophic factors from MEEs as detected with PCR) may be improving the efficiency of axonal regeneration, thereby obviating synkinesis. Future studies in large animal models will be needed to better understand the reproducibility and physiology involved.

3.5 Conclusion

Overall, we were able to show that a two-layer, muscle-cartilage implant integrates into host tissue with no foreign body inflammatory reaction. Additionally, we were able to improve function in a RLN injured larynx with a muscle implant induced to express motor endplates. Future studies in a large animal model will be needed to better assess the clinical applicability of this model.

3.6 Acknowledgements

These projects were supported in part by award number R01DC014070 from the National Institute on Deafness and Other Communication Disorders (NIDCD) within the National Institutes of Health (NIH). The content of this publication is solely the responsibility of the authors and does not necessarily represent the official views of the NIDCD or NIH. The authors would like to thank Melissa Bible and the rest of the Weldon School of Biomedical Engineering animal technical staff for their animal study support.

This study was performed in accordance with the Public Health Service Policy on Humane Care and Use of Laboratory Animals, the NIH Guide for the Care and Use of Laboratory Animals, and the Animal Welfare Act (7 U. S.C. et seq.); the animal use protocol was approved by the Purdue Animal Care and Use Committee.

3.7 References

1. SEER Stat Fact Sheets: Larynx Cancer USA: National Cancer Institute 2016 [Available from: http://seer.cancer.gov/statfacts/html/laryn.html.
2. Hamilton NJI, Birchall MA. Tissue-Engineered Larynx: Future Applications in Laryngeal Cancer. Current Otorhinolaryngology Reports. 2017;5(1):42-48.
3. Herrmann P, Ansari T, Southgate A, et al. In vivo implantation of a tissue engineered stem cell seeded hemi-laryngeal replacement maintains airway, phonation, and swallowing in pigs. J Tissue Eng Regen Med. 2017;1–12.
4. Macchiarini P, Jungebluth P, Go T, et al. Clinical transplantation of a tissue-engineered airway. Lancet. 2008;372:2023–2030.

5. Wambach BA, Cheung H, Josephson GD. Cartilage tissue engineering using thyroid chondrocytes on a type I collagen matrix. Laryngoscope. 2000;110(12):2008–11.
6. Kitani Y, Kanemaru S, Umeda H, Suehiro A, Kishimoto Y, Hirano S, et al. Laryngeal regeneration using tissue engineering techniques in a canine model. Ann Otol Rhinol Laryngol. 2011;120(1):49–56.
7. Long, J. L. Repairing the vibratory vocal fold. The Laryngoscope. 2018; 128: 153-159.
8. Fukahori, Mioko, Shun-ichi Chitose, Kiminori Sato, Shintaro Sueyoshi, Takashi Kurita, Hirohito Umeno, Yu Monden, and Ryoji Yamakawa. Regeneration of vocal fold mucosa using tissue-engineered structures with oral mucosal cells. PloS one. 2016; 11, no. 1: e0146151.
9. Ling, C., Li, Q., Brown, M.E., Kishimoto, Y., Toya, Y., Devine, E.E., Choi, K.O., Nishimoto, K., Norman, I.G., Tsegyal, T. and Jiang, J.J. Bioengineered vocal fold mucosa for voice restoration. Science Translational Medicine. 2015; 7(314), pp.314ra187-314ra187.
10. Kitamura, Morimasa, et al. Glottic regeneration with a tissue-engineering technique, using acellular extracellular matrix scaffold in a canine model. Journal of Tissue Engineering and Regenerative Medicine. 2016; 10.10: 825-832.
11. Brookes, S. , Voytik-Harbin, S. , Zhang, H. and Halum, S. Three-dimensional tissue-engineered skeletal muscle for laryngeal reconstruction. The Laryngoscope. 2018; 128: 603-609.
12. Paniello, R. C., Brookes, S. Bhatt, N. K., Bijangi-Vishehsaraei, K. , Zhang, H. and Halum, S. Improved adductor function after canine recurrent laryngeal nerve injury and repair using muscle progenitor cells. The Laryngoscope 128 (7), E241-E246, 2018.
13. Jonathan M. Fishman, BM BCh, MA, MRCS, Tahera Ansari, PhD, Paul Sibbons, PhD, FRCPath, Paolo De Coppi, MD, PhD, Martin A. Birchall MD Decellularized Rabbit Cricoarytenoid Dorsalis Muscle for Laryngeal Regeneration. FMedSci Annals of Otology, Rhinology & Laryngology. 2012; Vol 121, Issue 2, pp. 129 – 138.
14. Kanemaru, S. , Kitani, Y. , Ohno, S. , Shigemoto, T. , Kojima, T. , Ishikawa, S. , Mizuta, M. , Hirano, S. , Nakamura, T. and Dezawa, M. Functional regeneration of laryngeal muscle using bone marrow–derived stromal cells. The Laryngoscope. 2013; 123: 2728-2734.

15. Halum SL, Bijangi-Vishehsaraei K, Zhang H, Sowinski J, Bottino MC. Stem cell-derived tissue-engineered constructs for hemilaryngeal reconstruction. Ann Otol Rhinol Laryngol 2014;123:124–134.
16. Zhang, H. , Voytik- Harbin, S. , Brookes, S. , Zhang, L. , Wallace, J. , Parker, N. and Halum, S. Use of autologous adipose- derived mesenchymal stem cells for creation of laryngeal cartilage. The Laryngoscope. 2018; 128: E123-E129.
17. Suzuki, H. , Araki, K. , Matsui, T. , Tomifuji, M. , Yamashita, T. , Kobayashi, Y. and Shiotani, A. Value of a novel PGA- collagen tube on recurrent laryngeal nerve regeneration in a rat model. The Laryngoscope. 2016; 126: E233-E239.
18. Tan SS, Loh W. The utility of adipose-derived stem cells and stromal vascular fraction for oncologic soft tissue reconstruction: is it safe? A matter for debate. Surgeon. 2017;15:186–189.
19. Cousin B, Ravet E, Poglio S, et al. Adult stromal cells derived from human adipose tissue provoke pancreatic cancer cell death both in vitro and in vivo. PLoS ONE. 2009;4:e6278.
20. Mattsson P, Björck G, Remahl S, Bäckdahl M, Hamberger B, Hydman J, Svensson M. Nimodipine and microsurgery induced recovery of the vocal cord after recurrent laryngeal nerve resection. Laryngoscope. 2005;115(10):1863-5.
21. Rosen CA, Smith L, Young V, Krishna P, Muldoon MF, Munin MC. Prospective investigation of nimodipine for acute vocal fold paralysis. Muscle Nerve. 2014;50(1):114-8.
22. Sridharan SS, Rosen CA, Smith LJ, Young VN, Munin MC. Timing of nimodipine therapy for the treatment of vocal fold paralysis. Laryngoscope. 2015;125(1):186-90.
20 Avery, N. C. and Bailey, A. J. Enzymic and non- enzymic cross- linking mechanisms in relation to turnover of collagen: relevance to aging and exercise. Scandinavian Journal of Medicine & Science in Sports. 2005; 15: 231-240
23. Blum KM1, Novak T, Watkins L, Neu CP, Wallace JM, Bart ZR, Voytik-Harbin SL Acellular and cellular high-density, collagen-fibril constructs with suprafibrillar organization. Biomater Sci. 2016; Apr;4(4):711-23.
24. Gurtner GC, Werner S, Barrandon Y, Longaker MT. Wound repair and regeneration. Nature. 2008;453(7193):314-21.

25. Wong VW, Akaishi S, Longaker MT, Gurtner GC. Pushing back: wound mechanotransduction in repair and regeneration. The Journal of investigative dermatology. 2011;131(11):2186-96.
26. Vock VM1, Ponomareva ON, Rimer M. Evidence for muscle-dependent neuromuscular synaptic site determination in mammals. J Neurosci. 2008 Mar 19;28(12):3123-30.
27. Tan SS, Loh W. The utility of adipose-derived stem cells and stromal vascular fraction for oncologic soft tissue reconstruction: is it safe? A matter for debate. Surgeon. 2017;15:186–189.
28. Cousin B, Ravet E, Poglio S, et al. Adult stromal cells derived from human adipose tissue provoke pancreatic cancer cell death both in vitro and in vivo. PLoS ONE. 2009;4:e6278.
29. Sun B, Roh KH, Park JR, et al. Therapeutic potential of mesenchymal stromal cells in a mouse breast cancer metastasis model. Cytotherapy. 2009;11:289–298.

CHAPTER 4. LARYNGEAL RECONSTRUCTION USING TISSUE-ENGINEERED IMPLANTS IN PIGS: A PILOT STUDY

Previously published in The Laryngoscope. 2020 Nov 28. Epub ahead of print. PMID: 33247846.

4.1 Introduction

Devastating dysphonia or aphonia impacts thousands of individuals in the United States each year undergoing traumatic or oncologic partial laryngectomies.[1-2] Currently, there are no options for laryngeal reconstruction which add muscle volume and restore dynamic motion. Tissue-engineered myochondral implants (MIs) that are derived from the patient's own adult stem cells (via a biopsy under local anesthesia) and customized to address patient deficits would assist in addressing these unmet needs in laryngeal reconstruction. In addition, since the recurrent laryngeal nerve (RLN) may or may not be intact in these reconstructive scenarios, the ideal MIs would provide viable and functional reconstruction in environments with or without RLN integrity.

Over the past decade our laboratory has developed a novel method of constructing MIs with motor endplate-expressing muscle cells (MEEs) to promote innervation of MIs *in vivo*.[3-11] When the muscle cells are induced to express motor endplates, the cells release an array of neurotrophic factors (NFs); *in vivo*, these NFs promote axonal regeneration and innervation of the motor endplates, and associated muscle constructs.[10] Our group has also developed a patented unique self-assembling liquid collagen that, together with scalable biomanufacturing methods (e.g., extrusion, compression molding), is ideal for fabrication and customization of autologous MIs.[12-17] Our previous investigations using these MIs have been successful in a rodent model of partial laryngectomy. While "scaling up" has always been a tremendous hurdle in the field of laryngological tissue engineering, we herein report approaches to overcome this hurdle with resultant creation of large-volume MIs, adequate for reconstruction in a large animal model. Thus, the goal of the following investigations is to determine if autologous MEEs and ASCs can be used along with self-assembling collagen to create MIs that provide functional replacement for partial laryngectomy defects *in vivo* in a porcine model. Specifically, we will investigate if the MIs: (1) demonstrate strong innervation, adequate muscle volume and fiber

alignment/organization, and visible adductor activity; and (2) provide restoration of basic laryngeal protective reflexes for cough, swallowing, and airway maintenance over a follow-up period of up to 2 months.

4.2 Materials and Methods

4.2.1 Primary Muscle Progenitor Cell and Adipose Stem Cell Isolation and Culture

Yucatan minipigs (S&S Farms, Malta, IL) were anesthetized under isoflurane, and skeletal muscle and fat biopsies were obtained from the dorsal neck area. Fresh muscle and adipose tissue were minced in growth medium (GM); Dulbecco's Modified Eagle Medium (DMEM), 1% penicillin, streptomycin, amphotericin B (PSF-1, Hyclone, Logan, Utah) 20% fetal bovine serum (FBS, Hyclone, Logan, Utah), and digested in 0.2% collagenase type I (EMD Millipore, Temecula, CA) at 37°C for 2 hours. Digested muscle tissue was filtered through a 100-µm cell strainer, plated onto untreated 100-mm petri dishes (Fisher Scientific, Chicago, IL), and cultured overnight at 37°C with 5% CO_2. The supernatant was removed the next morning and transferred to culture flasks (Corning Life Sciences, Corning, NY). Digested adipose tissue was filtered through a 70-µm cell strainer and plated in a T-75 cell culture flask. Cells were cultured to 70% confluency and used in experiments at passages 1 to 2.

4.2.2 Fabrication of Engineered Skeletal Muscle Constructs

Muscle implants were fabricated as previously described.[3-10] Briefly, MPCs from biopsies were suspended in type I oligomeric collagen (GeniPhys, Zionsville, IN) (2.0 mg/mL) and flowed through a 10-mm cylindrical mold. Once polymerized, implants were cultured under passive tension in DMEM supplemented with 1% PSF-1, and 10% FBS at 37°C and 5% CO_2 for 2 days, with medium changes every 2 days. On day 3, medium was changed to differentiation medium, representing DMEM supplemented with 2% horse serum (HyClone) and 1% PSF-1, and constructs were cultured for an additional 5 days to induce myotube formation, at which point acetylcholine chloride (40 nM; Tocris Bioscience, Bristol, England), agrin (10 nM; R&D Systems, Minneapolis, MN), and neuregulin (2 nM; R&D Systems) were added to the medium to induce motor endplate formation. Constructs were cultured an additional 5 days with medium

changes every 3 days. Motor endplate expression was confirmed by immunostaining with Alexa Fluor 594 conjugated α-bungarotoxin (Molecular Probes, Eugene, Oregon).

4.2.3 Fabrication of Engineered Cartilage Constructs

Cartilage constructs were custom fabricated based on previously described methods.[10,12,17] Briefly, porcine ASCs were suspended in type I oligomeric collagen and polymerized. They were then compressed to constructs (412 mg total collagen, 3.4 cm in diameter, 5 mm in thickness) and cultured in chondrogenic differentiation medium (Hyclone Advance Stem Chondrogenic Differentiation Medium, SH30889.02; Thermo Scientific, Waltham, MA) and were maintained in a 37°C, 5% CO_2 incubator for 2 weeks. The medium was changed twice per week.

4.2.4 Fabrication of Engineered Vocal Fold Mucosa

Densified collagen scaffolds, custom fabricated using an adapted confined compression technique[12,14-16], were obtained from GeniPhys. Briefly, acid-soluble type I oligomeric collagen was neutralized and added to sterile cylindrical compression chambers. After collagen self-assembly, the resulting collagen scaffold was compressed to achieve a construct that was 315 mg in total collagen, 6.3 cm in diameter, and 0.55 mm in thickness. The construct was aseptically removed from the chamber and stored in sterile, sealed airtight containers prior to use in testing or surgery.

4.2.5 Partial laryngectomy, Recurrent Laryngeal Nerve Injury, and Reconstruction with the MI.

The animal study protocol was approved by Purdue Animal Care and Use Committee; institutional guidelines, in accordance with the National Institutes of Health (NIH), were followed for the handling and care of the animals. Three Yucatan minipigs were used for the experiments, all receiving cell-based implants. After three weeks of stem cell expansion and differentiation, the pigs underwent a partial laryngectomy surgery in which over a 3 cm^2 trans-mural defect was created, resecting the entire inner true vocal fold and false vocal fold with associated adductor muscle and outer supporting cartilage (Figure 4.1) with the defect extending

from the anterior commissure to the unilateral arytenoid. Only the arytenoid and overlying posterior laryngeal cartilage strut were spared on the reconstructed side to provide anchoring sites for the MI. Each layer was replaced with a tissue engineered implant: an acellular mucosa layer composed of densified collagen, a skeletal muscle layer composed of aligned oligomeric collagen and autologous MPCs differentiated and induced to express motor endplates (MEE), and a cartilage layer composed of densified oligomeric collagen and autologous ASCs differentiated to cartilage (Figure 4.1). Each layer was sutured to the thyroid cartilage using running 2-0 Vicryl. The left recurrent laryngeal nerve was ligated and a 1cm section removed. The subcutaneous tissue and skin were then closed with 2-0 Vicryl suture.

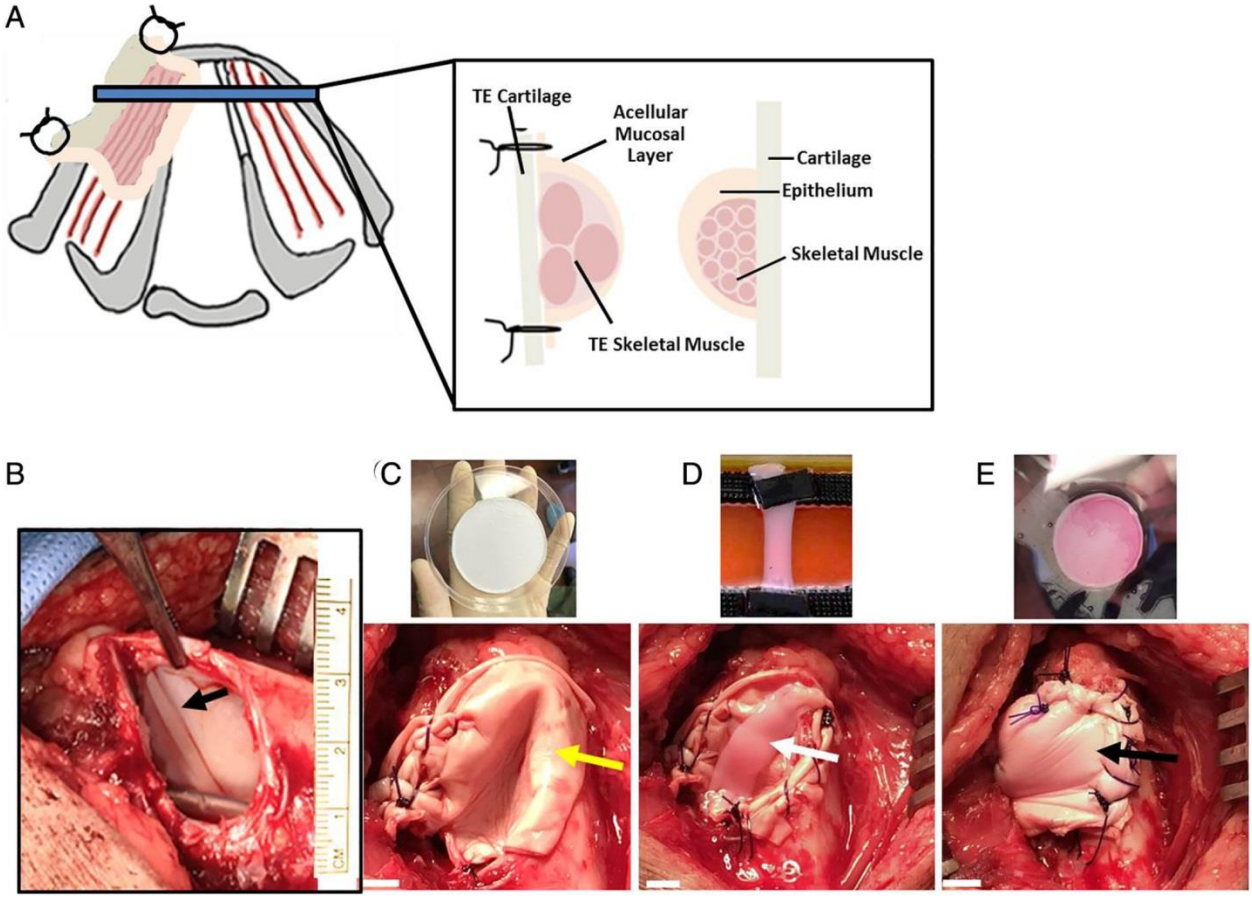

Figure 4.1: (A) Schematic drawing of left transmural laterovertical partial laryngectomy with tri-layer tissue engineered implants. The entire true vocal fold and false vocal fold were excised from the vocal process of the arytenoid to the anterior commissure, leaving only the arytenoid and small posterior thyroid cartilage strut as anchor points for the implant. Surgical Procedure: (B) Transmural surgical defect was created in left hemilarynx showing contralateral (right) vocal fold. (C) Mucosal sheet (acellular), (D) cellularized muscle, and (E) cellularized cartilage constructs before (top) and during (bottom) surgical implantation. Scale bars: 500μm

4.2.6 Videolaryngoscopy and Laryngeal Electromyography

At 2, 4 and 8 weeks after hemilaryngeal reconstruction, animals were returned to the operating room to be examined with videolaryngoscopy under anesthesia with inhalational isoflurane. Videolaryngoscopy was performed while titrating the anesthetic to permit stimulation-induced laryngospasm. The endotracheal tube (ETT) was briefly withdrawn and the videolaryngoscope was introduced orally. As needed, additional isoflurane anesthesia was provided via nosecone. The animals were assessed for stimulation induced laryngospasm (adduction) as well as spontaneous respiration related abduction. At the 8-week assessment, evoked laryngeal electromyography (LEMG) of the adductor complex was performed in addition to performing videolaryngoscopy during RLN stimulation. LEMG was performed with hooked wire electrodes placed in the right sided thyroarytenoid muscle or left sided engineered muscle while stimulating the ipsilateral RLN at the entrance into the larynx to determine firing patterns and recruitment of the MI muscle relative to that of the native laryngeal muscles. Despite the prior transection injury, the RLN fibers could be identified at the entrance in the larynx (near the cricothyroid joint) in all animals bilaterally. After videolaryngoscopy and LEMG were completed, the animals were euthanized while still under anesthesia according to NIH and ACUC-approved methods.

4.2.7 Voice data collection and analysis

Voice collected by 96k/24-bit Portable Stereo Recorder DR-05 (Tascam Linear). The recorder was placed approximately 50 cm directly in front of the pig's mouth and 60 second audio recordings were attained for each animal. The squeal is a long, high-pitched cry or noise that is the true sound from the vocal fold. The squeals of both pigs were recorded before the nerves were injured, and it was seen that the squeals occurred at a frequency of 2.0 kHz. "Audacity" was used to analyze the maximum amplitudes. Once the right RLN was severed, audio samples were taken every two weeks for a total of eight weeks.

4.2.8 Histological Assessment

After euthanasia, pig larynges and associated implants were harvested *en bloc* and fixed in 10% neutral buffered formalin and paraffin embedded. Sections were stained with

hematoxylin & eosin (H&E) and Mason's trichrome by the Purdue Histology Lab. Slides were viewed on a Nikon microscope (Eclipse E200, Nikon, Melville, NY) and images captured with a Leica camera (DFC480, Leica, Buffalo Grove, IL).

Muscle and cartilage constructs cultured *in vitro* were fixed in 4% paraformaldehyde overnight, and then transferred to 30% sucrose at 4^{o}C for an additional 24 hours. Cryosections (25-µm thickness) were prepared on a Thermo Cryotome FE (Fisher Scientific, Kalamazoo, MI). For histochemistry analysis, cryosections were washed with phosphate buffered saline three times, permeabilized with 0.1% Triton X-100 for 20 minutes, and then blocked with 1% bovine serum albumin for 2 hours. To stain for motor endplates and cytoarchitecture, slides were incubated with Alexa Fluor 594 (Molecular Probes) conjugated α-bungarotoxin (1:100) and Alexa Fluor 488 phalloidin (F-actin) respectively for 2 hours at room temperature. Slides were rinsed and mounted with Fluoro-Gel (Electron Microscopy Sciences, Hatfield, PA) for imaging on a Zeiss LSM 880 confocal microscope (Oberkochen, Germany).

4.3 Results

4.3.1 Videolaryngoscopy

Animals demonstrated appropriate weight gain, no aspiration events, and audible phonation, initially extremely soft and then gradually increasing in amplitude over time (see Table 4.1). Video laryngoscopy at 2, 4, and 8 weeks showed healthy, viable MI tissue, initially with exudate (week 2) at the anterior anastomosis, which was then gradually replaced with healthy mucosa and small granulomas at the anastomotic site (week 4), and by 8 weeks there was complete re-epithelialization with no induration or inflammation (Figure 4.2).

Table 4.1. Basic Acoustic Analysis of Porcine Phonation

Acoustic Properties	Immediately Preoperatively	Intermediate Postoperative Period (2 weeks)	Late Postoperative Period (8 weeks)
Relative Amplitude	1.00±0.15	0.54±0.03	1.06±0.11

To selectively analyze glottic phonation (rather than supraglottic noise), maximum amplitude for glottic phonation was analyzed at 2000 Hz, with 60 second audio recordings attained for each animal. Specifically, the amplitude of each glottic phonation was visualized and measured by Audacity software under waveform view (https://www.audacityteam.org/). The amplitude of each group was normalized by the normal glottic phonation obtained preoperatively.

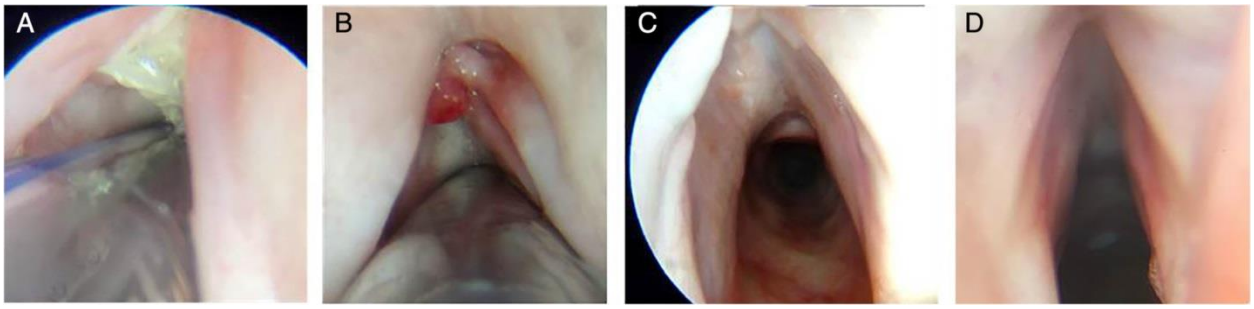

Figure 4.2: Representative endoscopic images of progressive healing of vocal fold mucosal surface on left side at (A) 2 weeks, (B) 4 weeks, and (C) 8 weeks following surgery compared to (D) normal. Vascularization and epithelialization are noted at 4 weeks. At 8 weeks, the mucosal surface appears completely healed and the implant is not identifiable within the airway lumen. Asterix indicates location of repair.

4.3.2 Histological Assessment

Histology confirmed re-vascularization of the implants supporting the observations of the viable tissue appreciated on videolaryngoscopy (Figure 4.3). The mucosal layer showed complete coverage with stratified squamous epithelium and vascularization along with glandular growth (Figure 4.4). The skeletal muscle layer showed complete integration, with good alignment and no inflammatory response (Figure 4.5). The cartilage layer showed significant neocartilage formation, with the implant portions adjacent to the native cartilage most closely replicating normal cartilage (Figure 4.6). Of particular interest was the finding that all three layers demonstrated complete integration of the engineered tissues not only with the native tissue but also with between MI layers, with no inflammatory foreign body reaction or rejection. Furthermore, the defect dramatically decreased in size over time, such that it became difficult to identify the original defect by 8 weeks because much of the MI became morphologically

indistinguishable from native tissue. Finally, as part of the histological analysis, the tissue engineered MIs were assessed for neuromuscular junctions via neuron (beta-3 tubulin) and motor endplate (α-bungarotoxin) immunohistochemistry which confirmed the presence of innervated neuromuscular junctions throughout the engineered muscle (Figure 4.7).

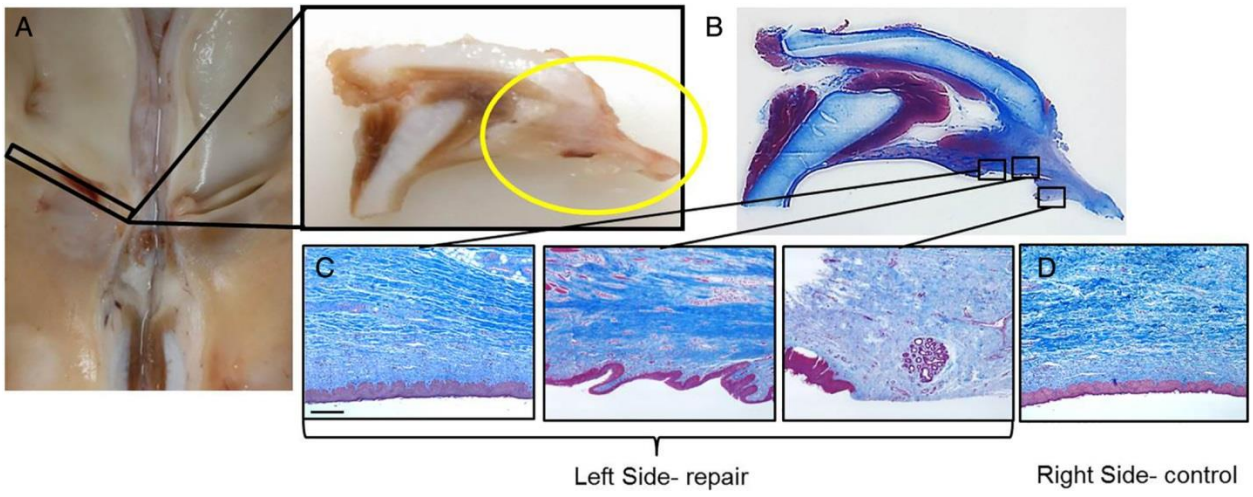

Figure 4.3: Regenerated mucosal epithelium as seen at 8 weeks in the post mortem larynx that is (A) unstained and (B,C) stained with Masson's Trichrome compared to normal (D). Yellow circle outlines location of original defect, much of which is grossly indistinguishable from the native hemilarynx now. Scale bar: 200μm

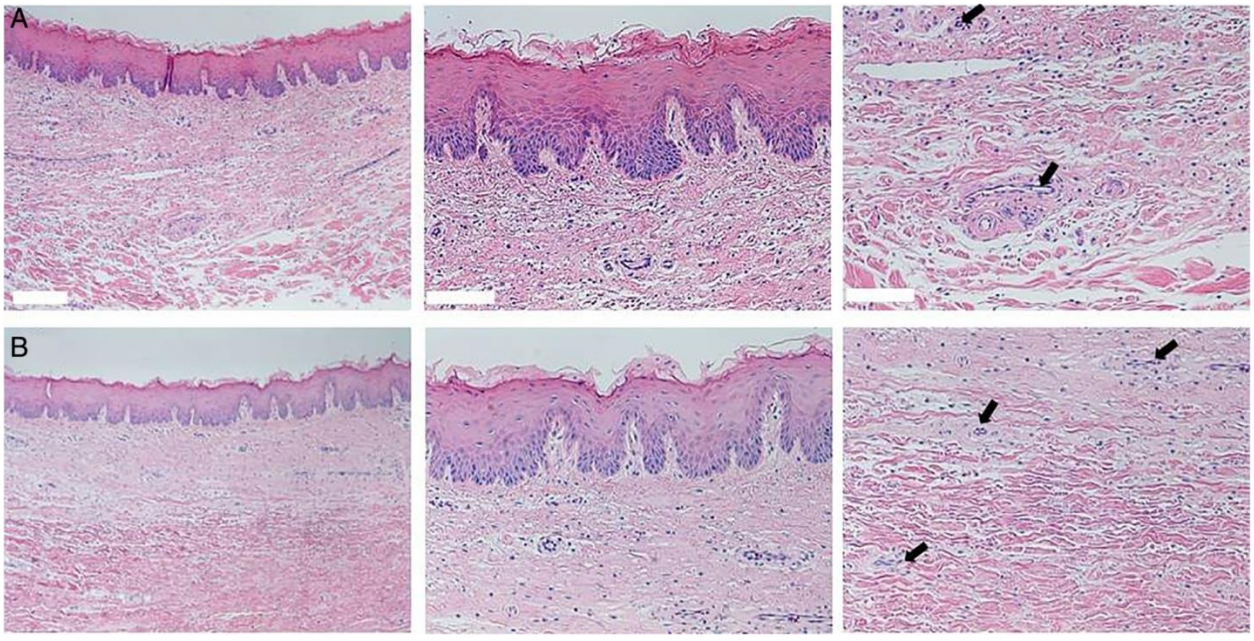

Figure 4.4: H&E staining of (A-C) mucosal layer showing regrowth of epithelium at 8 weeks following surgery compared to (D-F) untreated control. Arrows indicate vasculature. Scale bars: (A,D) 200μm; (B-C, E-F) 100μm

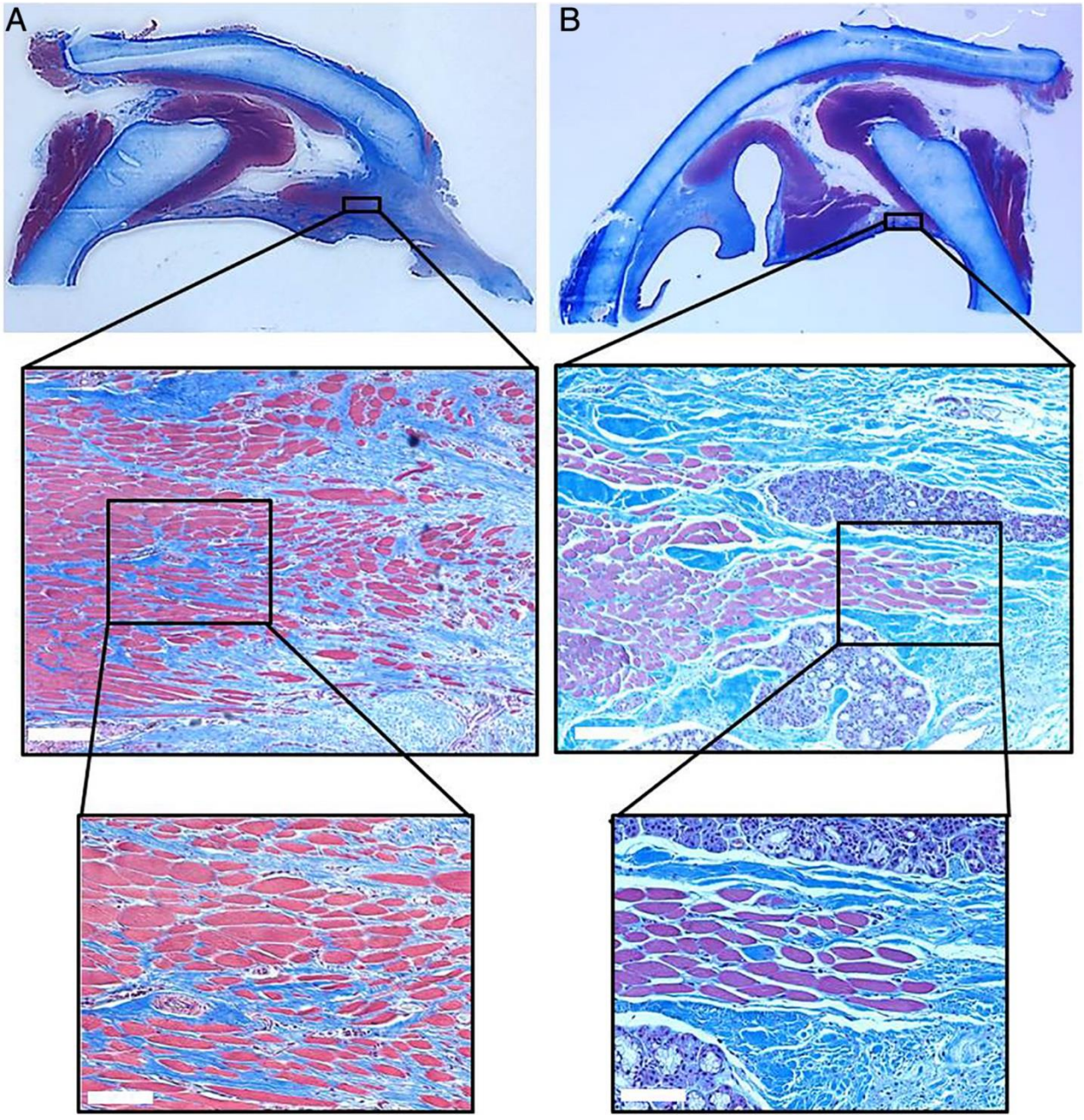

Figure 4.5: Masson's Trichrome stain of skeletal muscle interface in (A) reconstructed hemilarynx and (B) native control hemilarynx. Early stages of muscle regeneration are noted in the reconstructed larynx, with more mature skeletal muscle fibers noted in the untreated control.

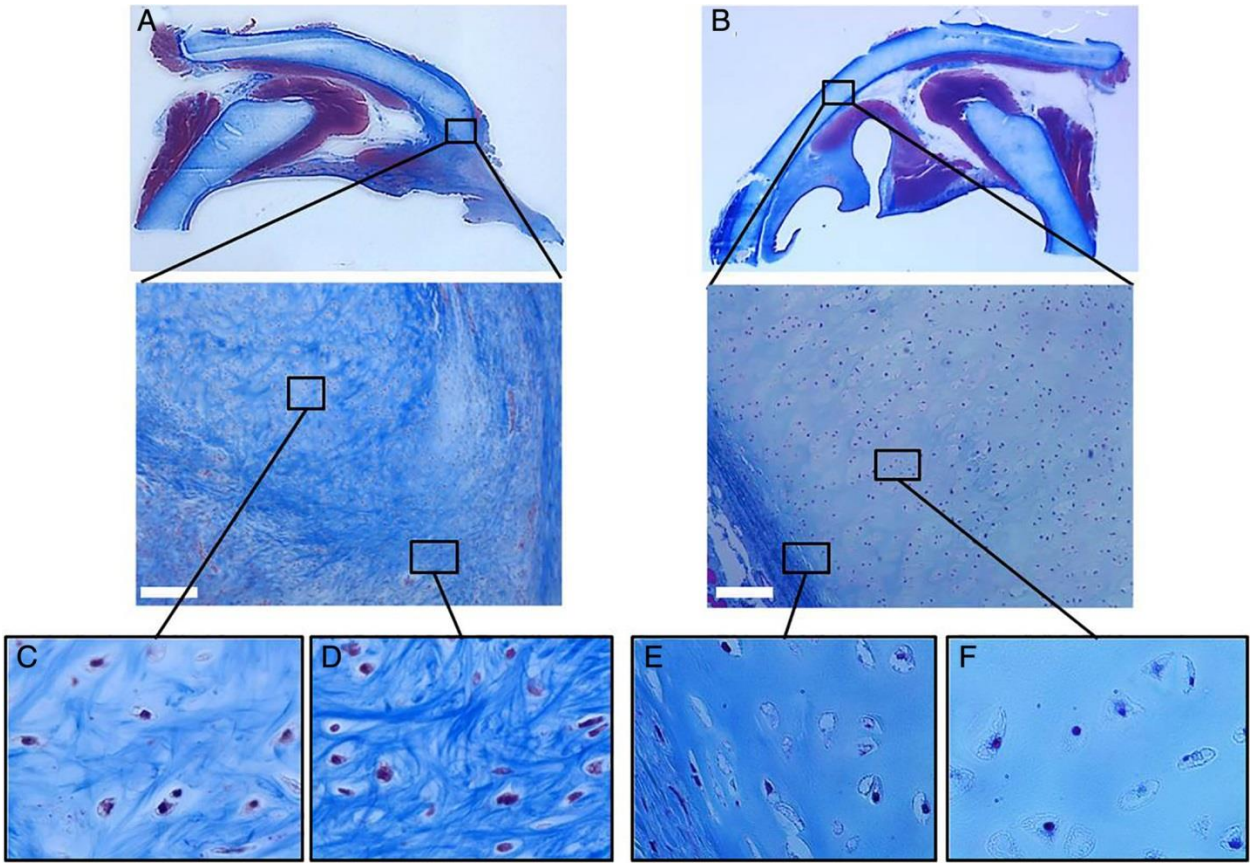

Figure 4.6: Masson's trichrome stain of cartilage interface in (A) reconstructed larynx and (B) untreated control. Neocartilage with different levels of maturation are evident within the reconstructed larynx, with (C) less dense collagen fibrils and cells within larger lacunae towards the center and (D) denser collagen fibrils with more cells within small lacunae found near the periphery. (E,F) Normal cartilage features chondrocytes within small lacunae surrounded by a highly uniform collagen matrix.

4.3.3 Laryngeal Electromyography

Evoked LEMG waveforms could be obtained bilaterally in all of the animals. At 8 weeks, the MEE implant animals also demonstrated visible adduction on direct RLN stimulation, while the acellular control animal actually demonstrated abduction but no clear adductor activity (Figure 4.7).

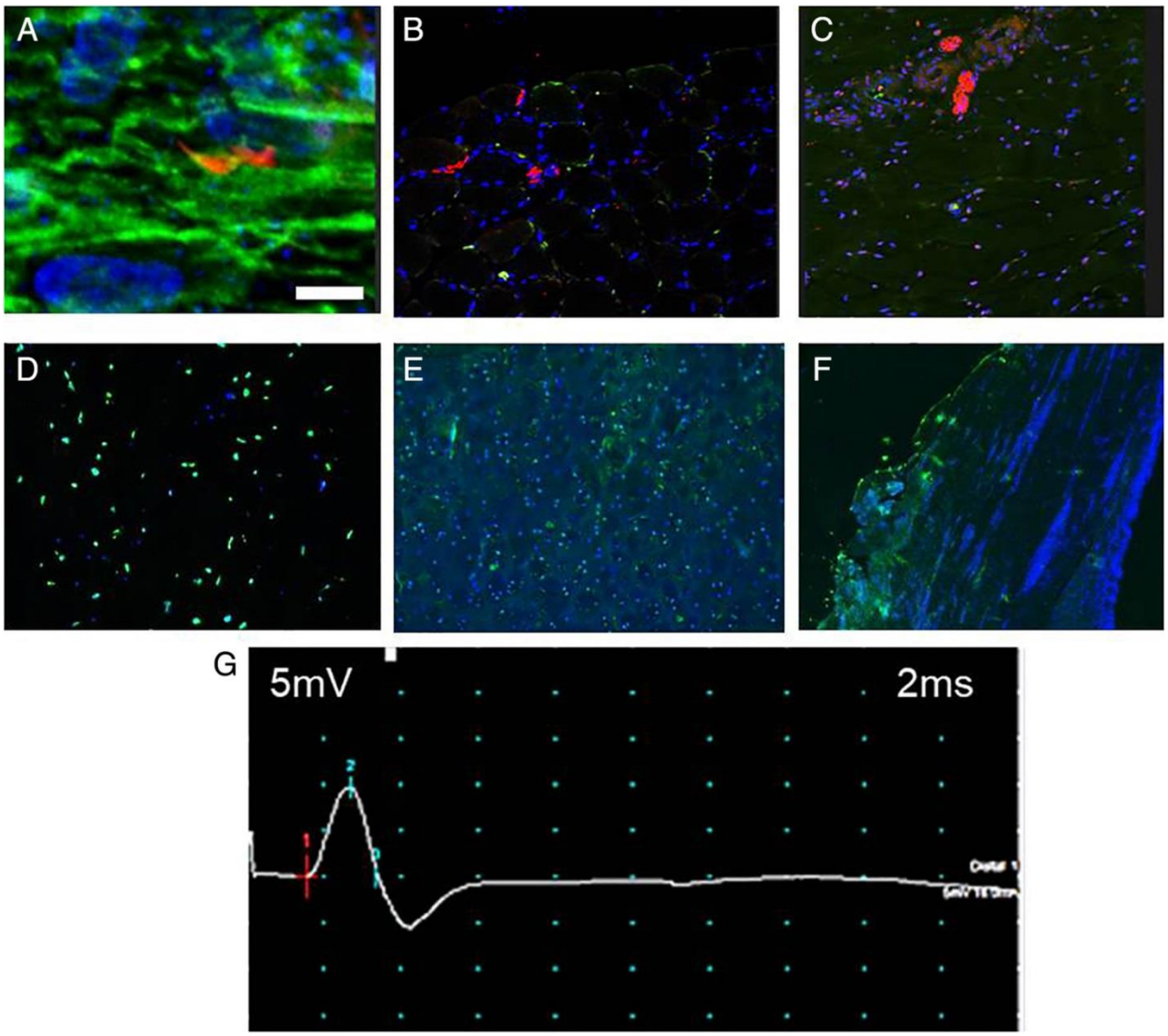

Figure 4.7: (A) In vitro MEE induction (Red- motor endplates, Green- F-actin, Blue- nuclei) (B,C) In vivo innervation (B: normal muscle, C: innervated implant; red: nerve fiber, green: motor endplate, blue: nuclei). (D) In vitro cartilage differentiation. (E, F) In vivo cartilage formation (E: normal cartilage, F: implant; green: collagen II, blue: nuclei). (G) Evoked LEMG with representative maximal stimulated motor unit action potential (MUAP) when transected RLN was stimulated distal to the point of injury shows early reinnervation in the MEE implanted animal at 8 weeks post-surgery. Scale bar: 100µm.

4.4 Discussion

Our previous investigations have used MIs to reconstruct the larynx in a rodent model of partial laryngectomy.[7,8,10,17] However, because the rodent larynx has a very small glottic airway and lacks protective reflexes such as cough, it is not a good model for transmural defects (only myochondral defects could be created). Considering that a transmural defect needs to be created to better simulate a neoplastic resection, these experiments focused on a large-animal

translational model involving the porcine larynx. Not only did this permit reconstruction of a transmural defect, but the porcine laryngeal anatomy and physiology also closely mimic that of the human larynx.[18,19] This initial porcine study demonstrates that autologous MEEs and ASCs can be used within unique self-assembling collagen to create MIs that provide restoration of basic laryngeal protective reflexes for cough, swallowing, and airway maintenance over a follow-up period of up to two months. Furthermore, we found that the MIs developed strong innervation, adequate muscle volume, and visible adductor activity on laryngoscopy, likely explaining the favorable post-surgical physiologic responses that the animals displayed.

While the ideal laryngeal replacement strategy has not been clearly established to date, there have been a wide variety of approaches including the concept of an artificial larynx[20] as well as the mesenchymal stem cell-coated decellularized larynx for laryngeal replacement.[21] Unfortunately, none of these investigational options add muscle volume and restore dynamic motion. As viable, aligned muscle is critical for restoration of laryngeal function, our laboratory has extensively studied approaches for engineering autologous laryngeal muscle,[7,8,10] and used the engineered muscle as the foundation for the MIs described in this study. Because of the complexity of the larynx and anatomic variability between animals, a multilayered construct was created so that each layer could be individually manicured/trimmed at the time of surgery, and then secured to the surrounding structures and other implant layers. The three layers included: (1) an acellular collagen vocal fold mucosa replacement (inner layer), (2) tubular MEE muscle long enough to layer upon itself (middle layer), and (3) an ASC-populated cartilage (outer layer). We removed the entire unilateral true and false vocal fold including the inner mucosa, adductor muscle and outer laryngeal cartilage–sparing only one arytenoid and a thin posterior laryngeal cartilage strut to facilitate anchoring the MIs. The engineered muscle was also secured in a manner such that the vector of muscle contraction would mirror that of the native adductors (running from the anterior commissure to vocal process of the arytenoid). Indeed, using this approach we have attained innervated engineered muscle with functional adduction based on videolaryngoscopy. Most importantly, the pigs have had no loss of function, maintaining airway, phonation, and swallowing (normal weight gain/no aspiration events). In fact, while phonatory quality was initially quite soft/breathy and weak in amplitude, the amplitude was actually restored to near-normal by 8 weeks.

While findings from the current investigation are encouraging, they are still very preliminary in nature. Future studies will be needed to adjust the MI structural integrity and function based on the size of the defect, and to create larger, possibly bilateral partial laryngectomy defects. Furthermore, other investigators such as Long et al[22] have been highly successful in tissue engineering vibratory mucosa to optimize voice quality, while our model used a nonvibratory collagen sheet for structural support. Thus, additional structural optimization will be important before clinical translation will become feasible.

4.5 Acknowledgements

The authors acknowledge assistance of V. Bernal-Crespo and the the Purdue University Histology Research Laboratory, a core facility of the NIH-funded Indiana Clinical and Translational Science, for preparation of histological slides. We also thank members of the Weldon School Preclinical Studies Research Team, including, M. Bible, T. Moller, G. Brock, T. Cleary, S. Nier, and R. Seiber, for all their time and effort related to animal husbandry and the animal study.

4.6 References

1. SEER Stat Fact Sheets: Larynx Cancer USA: National Cancer Institute 2018. Available at: https://seer.cancer.gov/statfacts/html/laryn.html.
2. Schaefer SD. The acute management of external laryngeal trauma A 27-year experience. Arch Otolaryngol Head Neck Surg. 1992;118(6):598–604.
3. Halum, S. L., Naidu, M., Delo, D. M., Atala, A. & Hingtgen, C. M. Injection of Autologous Muscle Stem Cells (Myoblasts) for the Treatment of Vocal Fold Paralysis: A Pilot Study: The Laryngoscope 2007;117, 917–922. PMID: 17473696
4. Halum SL, Hiatt KK, Naidu M, Sufyan AS, Clapp DW. Optimization of autologous muscle stem cell survival in the denervated hemilarynx. Laryngoscope. 2008;118(7):1308-12. PMID: 18401272

5. Halum SL, McRae BR, Bijangi-Vishehsaraei K, Hiatt K. Neurotrophic Factor-Secreting Autologous Muscle Stem Cell Therapy for the Treatment of Laryngeal Denervation Injury. Laryngoscope 2012;122(11):2482-96. PMID: 22965802
6. Hiatt K, Lewis D, Shew M, Bijangi-Vishehsaraei K, Halum SL. Ciliary Neurotrophic Factor (CNTF) Promotes Skeletal Muscle Progenitor Cell (MPC) Viability via the Phosphatidylinositol 3-kinase-Akt pathway. J Tissue Eng Regen Med 2014;8(12):963-8. PMID: 23147834
7. Halum SL, Bijangi-Vishehsaraei K, Zhang H, Sowinksi J, Bottino M. Stem Cell-Derived Tissue Engineered Constructs for Hemilaryngeal Reconstruction. *Annals of Otology, Rhinology & Laryngology*; 2014;123(2):124-34. PMID: 24574468
8. Brookes S, Voytik-Harbin S, Zhang H, Halum S. Three-dimensional tissue-engineered skeletal muscle for laryngeal reconstruction. Laryngoscope. 2018;128(3):603-609. PMID:28842993
9. Paniello RC, Brookes S, Bhatt NK, Bijangi-Vishehsaraei K, Zhang H, Halum S. Improved adductor function after canine recurrent laryngeal nerve injury and repair using muscle progenitor cells. Laryngoscope. 2018 Jul;128(7):E241-E246. PMID:29219186
10. Brookes S, Voytik-Harbin S, Zhang H, Zhang L, Halum S. Motor endplate-expressing cartilage-muscle implants for reconstruction of a denervated hemilarynx. Laryngoscope. 2019; 129:1293-1300.
11. U.S. utility patent application filed for PRF Ref. No. 67585 "Primed muscle progenitor cells and uses" (67585-02) with the United States Patent & Trademark Office (USPTO) on April 27, 2018
12. Blum, K. M. et al. Acellular and cellular high-density, collagen-fibril constructs with suprafibrillar organization. Biomater. Sci. 4:711–723 (2016).
13. Collagen Preparation and Method of Isolation. Inventors: Voytik-Harbin, S., Kreger, S., Bell, B., and Bailey, J., "Collagen Preparation and Method of Isolation." U.S. Patent 8,084,055, issued December 27, 2011, U.S. Patent 8,512,756, issued August 20, 2013.
14. Bailey JL, Critser PJ, Whittington C, Kuske JL, Yoder MC, Voytik-Harbin SL. Collagen oligomers modulate physical and biological properties of three-dimensional self-assembled matrices. Biopolymers. 2011 Feb;95(2):77-93. PMID: 20740490

15. Kreger ST, Bell BJ, Bailey J, Stites E, Kuske J, Waisner B, Voytik-Harbin SL. Polymerization and matrix physical properties as important design considerations for soluble collagen formulations. Biopolymers. 2010 Aug;93(8):690-707. PMID: 20235198
16. Novak T, Seelbinder B, Twitchell CM, van Donkelaar CC, Voytik-Harbin SL, Neu CP. Mechanisms and Microenvironment Investigation of Cellularized High Density Gradient Collagen Matrices via Densification. Adv Funct Mater. 2016;26(16):2617-28. PMID: 27346992
17. Zhang H, Voytik-Harbin S, Brookes S, Zhang L, Wallace J, Parker N, Halum S. Use of autologous adipose-derived mesenchymal stem cells for creation of laryngeal cartilage. Laryngoscope. 2018;128(4):E123-E129. PMID: 29238978
18. Blakeslee DB, Banks RE, Eusterman V, Brooks D. Analysis of vocal fold function in the miniswine model. J Invest Surg. 1995;8(6):409-24.
19. Gorti GK, Birchall MA, Haverson K, Macchiarini P, Bailey M. A preclinical model for laryngeal transplantation: anatomy and mucosal immunology of the porcine larynx. Transplantation. 1999;68(11):1638-42.
20. Debry C, Dupret-Bories A, Vrana NE, Hemar P, Lavalle P, Schultz P. Laryngeal replacement with an artificial larynx after total laryngectomy: the possibility of restoring larynx functionality in the future. Head Neck. 2014;36(11):1669-73.
21. Ansari T, Lange P, Southgate A, Greco K, Carvalho C, Partington L, Bullock A, MacNeil S, Lowdell MW, Sibbons PD, Birchall MA. Stem Cell-Based Tissue-Engineered Laryngeal Replacement. Stem Cells Transl Med. 2017;6(2):677-687.
22. Long J, Salinas J, Rafizadeh S, Luegmair G, Zhang Z, Chhetri D. In vivo vocal fold cover layer replacement. Laryngoscope. 2015;125(2):406-11.

CHAPTER 5. CONCLUSIONS AND FUTURE WORK

5.1 Summary

Laryngeal cancer is a treatable cancer with chemo- and radiation therapy coupled with complete or partial removal of the larynx. However, these treatments come with significant drawbacks of disfiguring scars, stomas, loss of voice, and inability to swallow. Current surgical options involve the use of autologous muscle or skin flaps that serve only to seal the airway and do not restore function. Thus, there is a need for a therapy that restores laryngeal function post cancer resection. This thesis has focused on tissue engineering the functional components of the larynx, namely the thyroid cartilage, thyroarytenoideus muscle, and the airway mucosa.

The early work focused on the skeletal muscle component. We showed that creating implants using type I oligomeric collagen and muscle progenitor cells produced aligned myofibers in vitro and were able to be induced to express motor endplates. Further, these were implanted into a rat model of hemilaryngectomy and integrated well into the host tissue.

Next, we combined this work with the cartilage engineering of Hongji Zhang to create myochondral implants for implantation into the rat. We were able to show integration into host tissue with evidence of new cartilage and muscle formation. Further, we were able to show improvement in laryngeal function with motor endplate expressing muscle implants.

With the successes of the rat studies, we moved to scale up the technology to a porcine hemilaryngectomy model, beginning with a proof-of-concept study in 2 pigs to describe the surgical technique of implanting all three functional layers (cartilage, muscle, mucosa).

5.2 Ongoing and Future work

Full characterization of the mechanical properties of the three tissue engineered layers (compression testing for cartilage, tensile testing for skeletal muscle, and suture retention and tensile testing for mucosa) is work that is currently ongoing. While some preliminary data is promising, more animal numbers are needed. We currently have a large-scale pig study in progress to further discover what contribution the cells have to cartilage regeneration at 1 month and 6 months. These studies will also determine what contribution the MEE implants have to reinnervation and return to function and phonation.

A large area of future work for this project involves the mucosa layer. This was originally designed for the purpose of maintaining a sealed airway and protection from airway pathogens. There is ample opportunity in future studies to optimize the mucosal layer for vibratory vocal fold characteristics and to design an implant to meet the design criteria of vocal fold tissue engineering.

Additionally, if we look beyond the world of laryngology, there are many opportunities to expand upon the work presented here. In particular, applying the skeletal muscle tissue engineering to volumetric muscle loss, applying the cartilage engineering to inflammatory or traumatic cartilage defects, and applying the mucosa engineering to aerodigestive and dental mucosal repair. Indeed, the engineering approaches herein described have broad potential for global applications in the human body.

PUBLICATIONS

1. Anti-acrolein treatment improves behavioral outcome and alleviates myelin damage in experimental autoimmune enchephalomyelitis mouse. G Leung, W Sun, L Zheng, S Brookes, M Tully, R Shi. Neuroscience 173, 150-155, 2011
2. Potassium channel blocker, 4-aminopyridine-3-methanol, restores axonal conduction in spinal cord of an animal model of multiple sclerosis. G Leung, W Sun, S Brookes, D Smith, R Shi Experimental neurology 227 (1), 232-235, 2011
3. Three-dimensional tissue- engineered skeletal muscle for laryngeal reconstruction. S Brookes, S Voytik- Harbin, H Zhang, S Halum. The Laryngoscope 128 (3), 603-609, 2018
4. Use of autologous adipose-derived mesenchymal stem cells for creation of laryngeal cartilage. H Zhang, S Voytik-Harbin, S Brookes, L Zhang, J Wallace, N Parker, S. Halum. The Laryngoscope 128 (4), E123-E129, 2018
5. Improved adductor function after canine recurrent laryngeal nerve injury and repair using muscle progenitor cells. RC Paniello, S Brookes, NK Bhatt, K Bijangi-Vishehsaraei, H Zhang, S. Halum. The Laryngoscope 128 (7), E241-E246, 2018.
6. Motor endplate-expressing cartilage-muscle implants for reconstruction of a denervated hemilarynx. S Brookes, S Voytik-Harbin, H Zhang, L Zhang, S Halum. The Laryngoscope 129 (6), 1293-1300, 2019
7. Laryngeal Reconstruction Using Tissue-Engineered Implants in Pigs: A Pilot Study. S Brookes, L Zhang, TJ Puls, J Kincaid, S Voytik-Harbin, S Halum. The Laryngoscope 2020
8. 3-dimensionial (3d) tissue-engineered muscle for tissue restoration. SL Voytik-Harbin, SL Halum, S Brookes, H Zhang US Patent App. 16/607,665 2020